

## The characteristics of millisecond pulsar emission: II. Polarimetry

Kiriaki M. Xilouris<sup>1</sup>, Michael Kramer<sup>2</sup>, Axel Jessner<sup>2</sup>, Alexis von Hoensbroech<sup>2</sup>, Duncan Lorimer<sup>2</sup>, Richard Wielebinski<sup>2</sup>, Alexander Wolszczan<sup>3</sup>, Fernando Camilo<sup>4</sup>

### ABSTRACT

We have made polarimetric monitoring observations of most of the millisecond pulsars visible from the northern hemisphere at 1410 MHz over a period of three years. Their emission properties are presented here and compared with those of normal pulsars. Although we demonstrated in paper I that millisecond pulsars exhibit the same flux density spectra and similar profile complexity, our results presented here suggest that millisecond pulsar profiles do not comply with the predictions of classification schemes based on “normal” pulsars. The frequency development of a large number of millisecond pulsar profiles is *abnormal* when compared with the development seen for normal pulsars. Moreover, the polarization characteristics suggest that millisecond-pulsar magnetospheres might not simply represent scaled versions of the magnetospheres of normal pulsars, supporting results of paper I. However, phenomena such as mode-changing activity in both intensity and polarization are recognized here for the first time (e.g., J1730–2304). This suggests that while the basic emission mechanism remains insensitive to rotational period, the conditions that, according to the canonical pulsar model, regulate the radio emission, might be satisfied at different regions in millisecond pulsar magnetospheres.

At least three types of model have been proposed to describe the millisecond pulsar magnetospheres, ranging from distorted magnetic field configurations due to the recycled nature of these sources to traditional polar-cap emission and emission from outer gaps. A comparison of the predictions of these models with the observations suggests that individual cases are better explained by different processes. However, we show that millisecond pulsars can be grouped according to common emission properties, a grouping that awaits verification from future multifrequency observations.

---

<sup>1</sup>National Astronomy and Ionosphere Center, Arecibo Observatory, P.O. Box 995, Arecibo, PR 00613, USA

<sup>2</sup>Max-Planck-Institut für Radioastronomie, Auf dem Hügel 69, 53121 Bonn, Germany

<sup>3</sup>Department of Astronomy and Astrophysics, Penn State University, University Park, PA 16802, USA

<sup>4</sup>Nuffield Radio Astronomy Laboratories, Jodrell Bank, Macclesfield, Cheshire SK11 9DL, England; Marie Curie Fellow

*Subject headings:* pulsars: millisecond — polarimetry — individual( J0613–0200, J0621+1002, J0751+1807, J1012+5307, J1022+1001, J1024–0719, B1257+12, J1518+4904, B1534+12, B1620–26, J1640+2224, J1643–1224, J1713+0747, J1730–2304, J1744–1134, B1744–24A, B1855+09, B1937+21, B1953+29, B1957+20, J2019+2425, J2051–0827, J2145–0750, J2229+2643, J2317+1439, J2322+2057)

## 1. Introduction

We have been monitoring the polarization characteristics of 24 millisecond pulsars (MSPs) at 1410 MHz for a period of three years, aiming at contrasting their emission properties and those of normal pulsars. Previous studies of individual MSPs have shown that their emission properties are complex (e.g., Thorsett & Stinebring 1990; Manchester 1992; Manchester & Johnston 1995; Navarro & Manchester 1996; Arzoumanian *et al.* 1996). This work provides the first approach in determining the systematics involved in the MSP emission properties, and compares them with the predictions of schemes based upon studies of normal pulsars (e.g., Rankin 1983a and Lyne & Manchester 1988).

At least three types of theoretical models have been developed to describe the magnetic field topology in MSP magnetospheres. This is a topic of considerable interest due to its impact on the evolutionary history and the statistics of this stellar population. Some models assume unusual magnetic field configurations for MSPs, due to the recycling which occurs during their evolution (Ruderman 1991; Chen & Ruderman 1993b). Other models constrain the non-dipolar magnetic field topology, by postulating vacuum electromagnetic radiation (Krolik 1991). In addition, the presence of higher order multipoles is severely constrained by the location of the spin-up lines as derived from magnetic torques (Arons 1993). A third class of model postulates emission resulting from outer magnetospheric gaps (e.g., Cheng, Ho & Ruderman 1986; Chen & Ruderman 1993a; Romani & Yadigaroglu 1995), or even a contribution of emission from traditional polar caps in addition to this process. While taking different approaches, these models sometimes predict only slight differences in the emission properties of the MSP magnetospheres. The predictions of these models are traced here using the largest sample of MSP polarimetry available so far.

The magnetic field configuration places constraints on pulsar evolutionary models, a subject of particular interest following the discovery of MSPs. High-quality polarimetric data potentially provide a means for determining the observed viewing geometry of a pulsar, namely the magnetic inclination  $\alpha$  and the line-of-sight trajectory  $\beta$ . Observationally, it is uncertain whether the magnetic inclination for normal pulsars evolves secularly on time-scales of  $\simeq 10^7$  yr (e.g., Lyne & Manchester 1988; Rankin 1992b; Bhattacharya 1992; McKinnon 1993). It is therefore a curious observation that there is a high percentage of pulsars with interpulses (IPs) or emission at low levels extending for a significant fraction of the pulsar period (signatures of orthogonal and aligned orien-

tation respectively), among the MSP population, composed primarily of very old objects. However, to determine whether this observation is significant, the systematics of MSP emission must first be well understood.

As an essential step towards meaningfully interpreting MSP data, it is vital to understand the systematics involved in their emission properties (spectra, intensity fluctuations, polarimetry and profile morphology). The present work, accompanied by a study of the profile shapes (Kramer *et al.* 1998a; hereafter paper I) and the location of the emission in MSP magnetospheres (Xilouris *et al.* 1998a; paper III), provide the first such systematic approach. In the following sections, the emission properties of 26 MSPs in total, 24 in our sample and two based on the available literature, are examined in the context of polar-cap emission as it is understood from extensive studies of normal pulsars (e.g. Rankin 1992b; Lyne & Manchester 1988; Gould 1994). The wide applicability of these classification schemes is discussed in view of the complex morphology and emission properties seen for MSP profiles (Section 3). The new trends identified in MSP profiles are summarized in Section 4, followed by a statistical analysis contrasting the properties of MSP and normal pulsars. The impact of physical conditions on MSP emission is examined in Section 5, where our results are discussed in the context of current theoretical models that attempt to describe MSP magnetospheres.

## 2. Millisecond-Pulsar Monitoring

Millisecond pulsar monitoring at 1410 MHz was initiated at the Effelsberg radio-telescope in April 1994 following a major upgrade of the associated data-acquisition hardware. These modifications were made to permit high time resolution observations (down to  $0.2\mu\text{s}$ ), and to increase the system stability, as required to study short-period pulsars. An adding polarimeter was used which accepts opposite-hand circularly polarized inputs at an intermediate frequency of 150 MHz, with a bandwidth of 40 MHz, through a network of hybrids followed by an on-line de-disperser. A full description of the polarimeter, the gain stability and the polarimetric calibration is presented by von Hoensbroech & Xilouris (1997).

During the three-year monitoring period, most of the sources presented in this work were routinely observed in 31 sessions, spaced about a month apart. During each run, the polarization properties of some well-studied pulsars (PSRs B1929+10, B0540+23, B1937+21 and B1855+09) were observed to enable the monitoring of instrumental cross-coupling. By incrementing the position angle of the  $\lambda 21$ —18 cm feed at Effelsberg, an offset parallactic angle is added to the input signal. A rapid variation of the *effective parallactic angle* (true parallactic angle + offset) is obtained in this way. This feature permits a quick determination of the instrumental cross-coupling phase and amplitude. Gain monitoring was achieved by injecting a calibration signal asynchronously with the pulsar period both before and after each scan. An extensive discussion of the calibration procedure is presented elsewhere (von Hoensbroech & Xilouris 1997).

The polarization profiles of most of the pulsars in our sample are presented in Figs. 1 through 6. Pulsars observed in total power mode only, such as PSR J2019+2425, or badly smeared profiles (e.g., B1937+21) are not presented here. The dispersion smearing is indicated by the resolution box on each profile. This time delay is computed for the central channel (i.e., bandwidth of 0.666 MHz centred at 1410 MHz) of the 60 de-disperser channels. The smearing correction applied to each individual channel is computed by a linear extrapolation of this central channel value.

### 3. A study of individual pulsars

As a pulsar rotates, different parts of its magnetosphere are swept across the observer’s line of sight. These parts are recognized as the components of emission that constitute the integrated profiles, which are known to exhibit considerable diversity in their morphology. Profile diversity has been addressed by a simplified picture (Rankin 1983a, b) which has served to explain the profile morphology of normal pulsars. Rankin proposes that two generic component types exist which combine in a systematic fashion to explain the diversity seen in normal pulsar profiles. Lyne & Manchester (1988) confirm this trend, but postulate a random rather than a deterministic process in which the components combine to form an integrated profile. Both models recognize that the spectral development as well as the polarization properties of the profile components vary with the location of a component within the integrated profile. It has been shown by Rankin (1983a) and confirmed by Lyne & Manchester (1988) that there is generally a difference in spectral index between the central and outer parts of the emission beam. The central part, associated with the “core” component in Rankin’s model, usually exhibits a steeper spectrum than the outer parts (or “conal” components), and is emitted from regions closer to the stellar surface (Rankin 1983a).

The level of circular polarization associated with the core component is often higher than at other longitudes, and exhibits a sense reversal within the core component. This property greatly assists in identifying the core components, features which are associated with central trajectories of the observer’s line-of-sight. The polarization position angle (PPA) of the linearly polarized component of radio emission ideally follows a curve described by the rotating vector model (Radhakrishnan & Cooke 1969, hereafter the RVM). In practice, the PPA curves often undergo sudden discontinuities from this predicted behavior (orthogonal modes) at certain pulse longitudes which correlate with drops in the intensity of the linear polarization. In most cases, when these orthogonal modes are accounted for (e.g. Stinebring *et al.* 1984) a PPA curve can be reconstructed and fitted with a curve described by the RVM. Complicated field topologies due to the recycled nature of MSPs (Ruderman 1991) and gravitational bending (e.g Pechenick *et al.* 1983; Chen & Ruderman 1993b) are just some of the effects expected to have influenced the MSP emission in near-surface emission models. Similar effects are anticipated if the emission originates from the proximity of the light cylinder. Here, magnetic sweep-back would influence both the profile structure and the PPA curve (Barnard 1986). In addition, the relativistic motion in a binary system is expected to affect, in a systematic fashion, the profile shapes and polarization characteristics (Damour & Taylor 1992)

of pulsars in such systems.

In this section, the polarization properties and profile development summarized above are traced for each MSP in our sample. PSRs B1937+21 and B1957+20 are also discussed due to their special emission properties, based on the literature available. A quantitative analysis of the polarization results is discussed in Section 4 and summarized in Table 1.

### 3.1. PSR J0613–0200

This MSP (Lorimer *et al.* 1995a) is a member of a low-mass binary system in a 1.2 day circular orbit. Its companion is likely to be a white dwarf of mass  $\approx 0.15M_{\odot}$ . The weak but systematic sense-reversing circular polarization at the profile centre suggests that this is a core component. The presence of such a component implies that the line of sight crosses the polar cap region near the magnetic axis, making a small impact angle  $\beta$ . At  $\lambda 21$  cm, normal pulsars with triple profiles, particularly those with wide profiles, preserve some amount of linear polarization, while PSR J0613–0200 is essentially unpolarized. Very little frequency development is seen in the profile morphology of this pulsar in contrast with the predictions for a triple profile. A basic triple symmetric structure is evident over a wide range of frequencies (Bell *et al.* 1997). One exception is evident in a low signal-to-noise profile at 780 MHz (Backer 1995), where the trailing component appears abnormally bright in comparison to the leading and core components. This *abnormal* development is not seen at higher frequencies. Typically, for normal pulsars, the central part of the profile exhibits a steeper spectrum than the outer components, and is thus expected to fade faster towards higher frequencies (Rankin 1993a). The observed minimal spectral evolution of the components is in contrast to the predictions of the Rankin model.

### 3.2. PSR J0621+1002

Being a member of a wide orbit binary system with a  $\approx 0.5M_{\odot}$  companion (Camilo *et al.* 1996a) this pulsar belongs to the proposed class of intermediate-mass binary pulsars. Its profile is among the widest known, and has a relatively sharp component towards the trailing edge, showing significant circular, and moderate linear polarization suggesting that this component could have been the profile core. Due to its displaced position in the profile, the classification of this component is therefore uncertain. The PPA curve is shallow and does not follow a RVM curve. The triple symmetric profile morphology remains unchanged between 370 MHz (Camilo *et al.* 1996a) and 1.4 GHz (Fig. 1), indicating *slow* spectral evolution of the components. The narrowing of the profile over this frequency range is also negligible, perhaps less than one degree.

### 3.3. PSR J0751+1807

This pulsar, recently detected at X-ray wavelengths (Becker *et al.* 1996) is in a short orbital period binary system, with a white-dwarf companion of  $0.15M_{\odot}$  (Lundgren *et al.* 1995). At 1.4 GHz, J0751+1807 displays a symmetric double-peaked profile. While the profile shape was stable throughout the three years of our observations, the polarization of its leading component varied. The linearly polarized intensity of the leading component fluctuates, while the associated PPA curve changes slope. In contrast, the PPA associated with the trailing profile component remains stable with time. The amount of circular polarization is small, and changes sense towards the trailing component. The profile of PSR J0751+1807 exhibits an *unexpected* frequency development. The 430-MHz profile (Lundgren *et al.* 1995) exhibits one bright leading component. In contrast to all expectations, at 1.4 GHz the trailing part develops into a distinct component which is brighter than the leading one. The profile width at 430 MHz is  $67^{\circ} \pm 3^{\circ}$ , while we measure a width of  $73^{\circ} \pm 6^{\circ}$  at 1.4 GHz. This is in good agreement with the 1.4-GHz profile presented by Lundgren *et al.* (1995), and also suggests insignificant profile narrowing within the errors of measurements. At both 430 MHz and 1.4 GHz, low-level emission is detected up to  $\approx 130^{\circ}$  in pulse longitude.

### 3.4. PSR J1012+5307

This field MSP is a member of a binary system (Nicastro *et al.* 1995), in a tight circular orbit with a low-mass ( $0.15M_{\odot}$ ) white-dwarf companion (Lorimer *et al.* 1995b; van Kerkwijk *et al.* 1996). It exhibits the most perplexing profile yet seen with at least nine components making up two or three separate structures (cf. paper I). A main pulse (MP) and a first interpulse (IPa) that resembles the MP in shape and polarization are followed by a third structure (IPb) which appears to be superposed on IPa. There is a strong resemblance between this profile and that of PSR B1055–52, a normal pulsar that is almost certainly an orthogonal rotator (Rankin 1983a). However, such a conclusion is far from obvious here, due to emission throughout most of the pulsar period. Moderate amounts of sense-reversing circular polarization are associated with both the MP and IPa, indicating the existence of core components in both structures. This suggests that even though their separation is only  $\Delta\phi_{\text{MP-IP}} = 70^{\circ}$ , they might result from a line of sight that crosses near two magnetic poles which are located less than  $180^{\circ}$  apart. Most likely, the MP and the IPb fit the classical MP – IP description, since their midpoint separation is close to  $180^{\circ}$ . However, emission at low levels continues throughout most of the pulsar period (e.g Nicastro *et al.* 1995), suggesting that all structures could as well originate from a single pole.

Assuming that the opening semiangles  $\rho$  of the beams of a MP and an IP are the same, the impact parameter of the IP follows from  $\beta_{\text{IP}} = 180 - 2\alpha - \beta_{\text{MP}}$ . Therefore, in the case of an orthogonal rotator, one expects  $\beta_{\text{IP}} = -\beta_{\text{MP}}$ . This directly reflects on the maximum rate of change of the PPA ( $\frac{\sin\alpha}{\sin\beta}$ ). Equal slopes for the PPA, but of opposite sign, should thus indicate an orthogonal rotator. While this should be a simple test, helpful in determining the viewing

geometry of pulsars with IPs, its value is questionable due to the ambiguity seen in the slopes of normal pulsars with IPs. In this case, equal slopes of the same sign for the MP and IPa, would indicate an aligned rotator, although we cannot exclude an ambiguous classification.

Observations of lower resolution at three frequencies (Nicastro *et al.* 1995) demonstrate an *abnormal* frequency development, with IPa exhibiting a much shallower frequency dependence than the outer structures. There is also little frequency dependence in the component separations, which is a property that has been previously regarded as indicating emission from different magnetic poles (Hankins & Fowler 1986). The low mass of the spectroscopically detected white-dwarf companion suggests an orbital inclination of  $\approx 67^\circ$ , close to an edge-on geometry. Assuming the angular-momentum axes of the binary system and the pulsar rotation are aligned, the suggested geometry is consistent with an orthogonal rotator. Such a geometry is further supported by RVM curve fits to the PPA of this pulsar, where  $\alpha \approx 88^\circ$ , and  $\beta \approx 5^\circ$  have been derived (paper III).

### 3.5. PSR J1022+1001

This pulsar is in a wide circular orbit with a  $\approx 0.87M_\odot$  companion (Camilo *et al.* 1996a). The emission is confined to a relatively narrow symmetric profile within which four or five sharp components can be fitted (paper I). Substantial circular polarization that exhibits a sense reversal identifies the central part of the profile with a core component. The linear polarization varies across the profile from essentially zero for the leading part, to a highly polarized, sharp trailing component. Profile and polarization variations have been identified where the leading and the trailing component alternate in strength. The relative intensity of the two components is seen to evolve at a rate inconsistent with pulsar mode changing, leading to two distinct profiles. The most common profile where the trailing component appears stronger than the leading component is shown in Fig. 2 annotated as (A), while the less frequent one which also exhibits a much sharper PPA is annotated as (B). The PPA curve is often disturbed by orthogonal mode-changing. However, when these discontinuities are accounted for by applying appropriate shifts, the PPA closely follows an RVM curve. A fit of the RVM curve to the PPA curve for this pulsar yields  $\alpha \approx 53.2^\circ$ , and  $\beta \approx 7.3^\circ$  (paper III). From this viewing geometry, we were able to estimate the emission height of the radio-emitting region. Assuming a dipolar magnetosphere, the height is consistent with  $3.2 R_*$ . At 430 MHz, pulse shape variations are also seen, while at 1.7 GHz, the leading component is brighter most of the time (Camilo *et al.* 1998). At 4.85 GHz (Kijak *et al.* 1997), the trailing component has faded with respect to the leading one. Between 430 MHz and 4.85 GHz, the profile development is *not consistent* with that of a triple or multiple profile. It is atypical of MSP profiles to exhibit the secular variations found in this source.

### 3.6. PSR J1024–0719

This recently discovered isolated pulsar (Bailes *et al.* 1997) exhibits a multi-component profile with high linear and moderate amounts of circular polarization associated with the central component. Comparing with lower frequency profiles (Bailes *et al.* 1997), the central component has gained in intensity at higher frequencies. If this is associated with the core component, then the spectral evolution is *contrary* to that expected for a pulsar of this type.

### 3.7. PSR B1257+12

This pulsar, the central object of the first extra-solar planetary system to be discovered (Wolszczan & Frail 1992), exhibits a very high degree of circularly polarized emission with sense reversal. This indicates the presence of a core component in the centre of the profile, implying that the line-of-sight cuts the polar cap close to the magnetic axis. The high degree of linear polarization is consistent with the highly polarized core components seen in the core-single profiles of normal pulsars. There is no significant narrowing of the profile between 430 MHz (Wolszczan & Frail 1992), 790 MHz (Backer 1995), and 1.4 GHz, *nor is there a significant* morphological development. The core component is brighter at 430 MHz, but has faded and becomes comparable in intensity to the trailing profile component at 1.4 GHz. This is in good agreement with the development of a triple profile. The PPA swing is shallow but well defined, and in agreement with a dipolar magnetosphere for this pulsar.

### 3.8. PSR J1518+4904

This pulsar, which has the longest period in our sample, is in a wide orbit around a  $\approx 1.0M_{\odot}$  companion which is probably another neutron star (Nice, Sayer, & Taylor 1996). A post-cursor component has possibly been identified (paper I) following the main pulse by  $25^{\circ}$ . The two features are connected with very low-level emission. Moderate levels of linear polarization and circular polarization that preserves one sense are seen, while the PPA is well defined and has a shallow slope. The spectral evolution of the profile components is *negligible* between the 370-MHz discovery profiles and our measurements.

### 3.9. PSR B1534+12

The profile of this pulsar has been extensively studied by Arzoumanian *et al.* (1996) at 430 MHz and 1.4 GHz. The MP has a multiple component shape with a total width of  $7^{\circ}$  at 10 % of maximum, including a surprisingly sharp component of  $\approx 2.5^{\circ}$  width. With its moderate levels of linear polarization, and sense-reversing circular polarization, this component is an exceptionally



narrow feature, unexpected in the context of a canonical model. There is also low-level emission present throughout a significant fraction of the period. The PPA curve is well defined, and the orientation presented by Arzoumanian *et al.* (1996) is consistent with an orthogonal rotator. PSR B1534+12 is a member of a NS-NS binary system and thus one of the few cases where general relativity predicts a measurable precession. The precession rate predicted for the spin axis of B1534+12 amounts to  $0.52^\circ\text{yr}^{-1}$ . Over the two years between our observations (April 1994) and those presented by Arzoumanian *et al.* (1996), such a small rate would imply a change in the PPA curve slope of  $\approx 1^\circ$ , assuming that the spin and orbital angular momentum axes of this binary system are aligned. Though high signal-to-noise observations are needed to detect precession, our data do not present indications that contradict the predictions of relativity for this system. We have used the orientation of this pulsar to derive the emission altitude, and estimate values of 30 and  $47R_*$  for the two solutions presented by Arzoumanian *et al.* (1996). There is *very little* change in profile morphology with frequency with both the MP and the IP fading very little relative to their conal outriders. The MP and IP do not fade relative to each other with frequency. In normal pulsars, IPs are rarely evident above 1.4 GHz.

### 3.10. PSR B1620–26

This pulsar is a member of a triple system (Backer *et al.* 1993) located in the globular cluster M4 (Lyne *et al.* 1988). Its pulse profile is symmetric, and perhaps the easiest to interpret in our sample since the emission characteristics of the core component are clearly evident. The high degree of circular polarization associated with significant linear polarization and a well defined PPA curve indicates the existence of a core component between two conal outriders. Comparing the 408-MHz (Lyne *et al.* 1988), 790-MHz (Backer 1995), and 1300-MHz (Foster *et al.* 1991) profiles with our 1.4-GHz measurements, there is *no significant* frequency development in shape or width of the profile.

Since B1620–26 was born in a globular cluster, it may not share the same genesis as the field pulsars which dominate our sample. Despite the expected modification of the field topology around the magnetic axis by a prolonged accretion process (Chen & Ruderman 1993b), we see no evidence to support different observational characteristics for the emission properties of this pulsar from the rest of the sample.

### 3.11. PSR J1640+2224

This MSP is a member of a binary system with a  $\approx 0.3M_\odot$  companion in a wide circular orbit (Foster *et al.* 1995). It exhibits a wide, multi-component profile (paper I) with high linear polarization and moderate circular polarization associated with the profile centre. The PPA curve is strikingly flat. In a sample of  $\approx 300$  polarimetrically studied normal pulsars (Gould 1994), five

sources have been identified with PPAs flatter than  $\left| \left( \frac{d\psi}{d\phi} \right)_{\max} \right| \leq 0.5 \left( \frac{\text{deg}}{\text{deg}} \right)$ . These sources (e.g. PSR B0031-07, B0940+16, B1809-176, B1822-14 and B2011+38) have single component profiles which preserve their simple shape at higher frequencies, consistent with conal-single profile development. Conal-single profiles are associated with trajectories of the line of sight that almost graze the emission cone. For these five sources, fits to their PPA of a RVM predict a normalized impact parameter between 0.94 and 0.98, which indeed signifies very tangential trajectories. Despite the flat PPA curve, PSR J1640+2224 does not share a similar profile development with these sources. Instead, profile outriders are evident at  $\lambda$  21cm, suggesting that the profile is consistent with a core surrounded by a pair of conal outriders. Triple profiles are associated with central trajectories and hence much steeper slopes than the extremely flat one found here. Thus, the flat PPA is difficult to understand within the same framework which applies to normal pulsars. Mutlifrequency and high resolution observations are essential in understanding this pulsar.

### 3.12. PSR J1643–1224

This source is among the most luminous MSPs known. It is a member of a binary system, with a  $\approx 0.14M_{\odot}$  companion in a wide circular orbit (Lorimer *et al.* 1995a). The wide profile resembles the triple core-dominated profile often seen amongst the normal pulsars. The moderate degree of linear and significant circular polarization seen here are properties often associated with single core component profiles. This suggests that our line-of-sight cuts the polar cap very close to the magnetic axis, although the PPA curve is rather flat for such a geometry. A very *slow* frequency development is noticed for this profile.

### 3.13. PSR J1713+0747

This field MSP is in a wide circular orbit around a  $\approx 0.3M_{\odot}$  companion (Foster *et al.* 1993). The pulsar’s large flux density and sharp profile make it an excellent source for high-precision timing experiments (Camilo *et al.* 1994a). Kijak *et al.* (1997) recently reported the detection of this pulsar at 4.85 GHz. At 1.4 GHz, the profile can be separated into at least five components (paper I). Sense-reversing circular polarization within the sharp central component identifies this with the core component. The leading part of the profile, where additional components can be fitted, is only weakly polarized, and the PPA curve is disturbed by  $90^{\circ}$  discontinuities. Such discontinuities tend to correlate with sudden drops of the linearly polarized intensity. These orthogonal emission modes have long been held responsible for the depolarization of pulsar radio emission. The PPA curve, when reconstructed for the orthogonal mode, is rather flat. At 430 MHz, the trailing part of the profile is intrinsically broadened (Foster *et al.* 1993). Between 1.4 and 4.85 GHz, no significant profile development is observed, although the outermost components are somewhat more prominent at 4.85 GHz than at lower frequencies.

### 3.14. PSR J1730–2304

This isolated MSP (Lorimer *et al.* 1995a) exhibits a multi-component profile at 1.4 GHz. Changes in the profile shape, similar to the mode-changing activity known from normal pulsars, have been identified (Kramer *et al.* 1998b). Different profile shapes are associated with changes in the degree of linear polarization, ranging from completely polarized to essentially unpolarized. This peculiar behavior mainly affects the observed linear polarization, while the circular polarization appears stable. From the polarization profiles, we also find sudden drops in the linear polarization which are associated with  $90^\circ$  discontinuities in the PPA curve. A small amount of sense-reversing circular polarization seems to be associated with a central core component, indicating that our line-of-sight cuts the polar cap very close to the magnetic axis. A post-cursor has been detected (paper I), which follows the main pulse by  $\approx 120^\circ$ . The two features are most likely not connected by low-level emission, though future observations at lower frequencies might be more informative.

### 3.15. PSR J1744–1134

This isolated MSP (Bailes *et al.* 1997) exhibits an interesting profile. High signal-to-noise profiles presented in paper I reveal a pre-cursor preceding the MP by  $\approx 124^\circ$ , as well as a trailing component following the profile by  $\approx 80^\circ$ . Moderate amounts of linear and circular polarization are seen. The PPA is well defined and of steep slope compared with the slopes derived for the majority of our sources. The PPA agrees well with the predictions of a RVM (paper III). *Very little* morphological change with frequency is seen for this profile.

### 3.16. PSR B1744–24A

Located in the globular cluster Terzan 5, this is the second globular cluster pulsar in our sample (cf. PSR B1620–26). PSR B1744–24A is an interesting source as its emission is eclipsed by a binary companion (Lyne *et al.* 1990). The emission exhibits significant amounts of linear polarization, whose degree is a function of orbital phase and is varying between 60% and essentially zero. The associated circular polarization remains constant (see Xilouris *et al.* 1998b *in prep.* for more details). The PPA curve is well defined with a shallow slope.

### 3.17. PSR B1855+09

The detection of a Shapiro delay in the timing data of this relativistic binary system (Ryba & Taylor 1991) indicates its orbital plane is roughly parallel to the line-of-sight, implying that PSR B1855+09 is most likely an orthogonal rotator (Thorsett & Stinebring 1990). The separation  $\Delta\phi_{\text{MP-IP}}$  is  $192^\circ$ . However, the fit of a RVM to the PPA curve (Segelstein *et al.* 1986) does

not provide conclusive evidence as to whether the IP is produced at the same or the opposite magnetic pole to the MP. Comparing the  $\Delta\phi_{\text{MP-IP}}$  at 430 MHz (Thorsett & Stinebring 1990), 3 GHz (Foster *et al.* 1991) and 4.85 GHz (Kijak *et al.* 1997), shows that there is no significant change with frequency, suggesting that the MP and the IP originate from two separate magnetic poles (cf. Hankins & Fowler 1986).

The sense-reversing circular polarization detected under the central part of the MP indicates the existence of a core component. A similar effect also occurs for the IP, implying that both the MP and the IP are created by a cut of the line-of-sight close to two different magnetic poles, further supporting an orthogonal geometry. We note that the polarization properties of the interpulse derived from our data are very similar to those presented by Segelstein *et al.* (1986). The linear polarization does not drop to zero at the pulse longitude where the PPA curve exhibits discontinuities, in good agreement with the measurements of Segelstein *et al.* (1986). The discontinuities observed in our data are non-orthogonal, which suggests that there is competition between modes of different intensity. This could account for the slight change in the percentage linear polarization observed among different sessions, or shorter integrations of the same session. The frequency development of the IP is *unusual* since at higher frequencies it is stronger relative to the MP (Kijak *et al.* 1997). Extended low-level emission has been reported only by Segelstein *et al.* (1986). If confirmed, this would be of interest since it cannot be reconciled with the strong case presented here for an orthogonal rotator.

### 3.18. PSR B1937+21

Our observations of this pulsar are in agreement with previously published polarimetry. However, due to hardware limitations, the time resolution is poorer and we do not present them here and the following discussion is based on the available literature. The profile of PSR B1937+21 consists of a MP, which has at least two components closely spaced to each other, and an IP. The separation  $\Delta\phi_{\text{MP-IP}} = 174^\circ$  remains constant for a wide frequency range, from 0.32 up to 2.38 GHz (see Ashworth *et al.* 1983; Stinebring & Cordes 1983; Cordes & Stinebring 1984; Thorsett & Stinebring 1990; paper I). The constant  $\Delta\phi_{\text{MP-IP}}$  could be perceived as an indication that the emission originates from two different magnetic poles. This view is further supported by the lack of low-level emission for most of the period, at least with the current observations (e.g. Camilo 1995). The MP and the IP are both sharp features, much narrower than the predictions of the canonical pulsar model, while their width is strongly frequency dependent. The profile development is normal and rather a weak function of frequency. The amplitude ratio of the MP and IP, contrary to the behavior seen in other MSPs with IPs, remains stable with frequency. Following the trend already recognized in other MSPs, the PPA curve of this star is very flat across both the MP and the IP while signatures of orthogonal moding are evident at the leading edge of the MP (e.g. Thorsett & Stinebring 1990). The linear polarization of the MP ranges from 64 % at 430 MHz to 18 % at 2.38 GHz (Thorsett & Stinebring 1990). Therefore, the emission properties of this pulsar are not

significantly different from those of a normal pulsar. Consequently, its magnetosphere might not be deviating from a dipolar structure that characterizes normal pulsars. However, the sharpness of its components remains a great puzzle. Cordes & Stinebring (1984) suggest that the emission region of PSR B1937+21 must be very compact. The lack of detectable non-dispersive time delays in pulse arrival suggests that all emission from 0.3 to 1.4 GHz must arise from the range of radii  $\Delta r=2$  km.

Emission from a single pole, located very near the stellar surface, has been suggested by Gil (1983) for this pulsar. In this model the contribution of the quadrupolar field component to the total magnetic field significantly alters the emission properties. Along similar lines, complex field topologies in polar caps modified by accretion during the spin-up or spin-down phase of the evolution of this star have been held responsible for the sharp features and the flat PPA curve observed (Chen & Ruderman 1993b). While the fashion in which complex fields influence the emission remains unclear (e.g. Krolik 1991), the emission properties of this pulsar are not so different from normal pulsars.

### 3.19. PSR B1953+29

Although this pulsar was rather weak during our observations, we were able to confirm the existence of the *pre-cursor* reported by Thorsett & Stinebring (1990). This feature precedes the main pulse by  $120^\circ$ . Boriakoff *et al.* (1986) found no evidence for an interpulse at lower frequencies, while Stinebring *et al.* (1984) found no significant polarization. Our polarization measurements generally agree with those of Thorsett & Stinebring (1990), although we observe some variability in the degree of polarization. This could explain the non-detection of polarization by Stinebring *et al.* (1984). Similarly, variability in intensity could be responsible for the non-detection of the precursor at 430 MHz. The frequency development of this pulsar is certainly *unusual* since the trailing part of the relatively simple profile at 430 MHz evolves to a three-component profile at 1.4 GHz (paper I).

### 3.20. PSR B1957+20

The eclipsing binary pulsar B1957+20 exhibits the most puzzling emission properties among all MSPs. Despite our persistent efforts we were unable to detect this source. However, for the sake of completeness, a discussion of its properties is presented here based on the available literature. The profile of PSR B1957+20 consists of a MP (nomenclature of Thorsett & Stinebring 1990) which resembles a core-single profile. A rather broad and asymmetric IP is located almost  $180^\circ$  from the MP. This component exhibits the most unusual profile development among the known pulsars (Fruchter *et al.* 1990). Low-level emission connects these two components, while two additional baseline-features have also been detected. Both features precede the MP and the IP structure

by about  $40^\circ$  (Fruchter *et al.* 1990). While the MP resembles a core-single profile, its frequency development is minimal (Thorsett *et al.* 1989), in contrast to the predictions for this profile class. On the contrary, the frequency development of the IP does not agree with the predictions of Rankin’s classification scheme. There is a substantial difference between the low and high frequency profile of this component. The baseline-features appear stronger at low frequencies while their spectral development is minimal as well. The polarization properties of this pulsar remain unknown and as suggested by Thorsett & Stinebring (1990), they are influenced by the environment of this eclipsing system. Theoretical arguments strongly suggest that this pulsar is an orthogonal rotator, making the origin of all the profile features an interesting puzzle.

Similar to B1937+21 the width of the MP of B1957+20 is much narrower than expected. Therefore, the discussion presented for the profile of B1937+21 might apply for the MP of B1957+20. However, this does not apply to the IP. The properties of this component are totally abnormal. The MP develops with frequency as expected in a traditional polar cap environment. On the contrary, the IP is far from this description. Further observations are required to establish whether the emission region of the IP might stem from a totally different location than the MP. Its much wider profile suggests that the IP might emanate from the vicinity of the light cylinder. If this is the case, then the abnormal profile properties should be associated with emission from outer magnetospheric gaps. The profile asymmetries of the IP, as well as the extra baseline components could emerge as the magnetic field lines at the vicinity of the light cylinder acquire an azimuthal component, guiding the emission at wide angles from the IP. The low degree of polarization detected at 430 MHz (Fruchter *et al.* 1990) can not readily assist in verifying the origin of the MP and IP of this source, however, such observations are needed to clarify this issue.

### 3.21. PSR J2019+2425

This pulsar is a member of a binary system (Nice *et al.* 1993) orbiting a  $\approx 0.37M_\odot$  companion. Due to severe scintillation, PSR J2019+2425 is one of the most difficult sources to study. However, it exhibits a perplexing profile and hence is included in our discussion which is based on data presented by Nice (1992). The MP is comprised of two main components, A and B, following the nomenclature of Nice (1992). A precursor (PC, component C) precedes the MP, while an almost symmetrically spaced possible IP or postcursor (component D) follows. Defining the profile center as the midpoint between component A and B, the IP follows the MP by  $\Delta\phi_{\text{MP-IP}} \approx 123^\circ \pm 7^\circ$  at 430 MHz, a separation that marginally narrows to  $\approx 116^\circ \pm 7^\circ$  at 1.38 GHz. Some evidence for the IP was also found in our 1.4 GHz data (paper I). The PC precedes the MP by  $\approx 104^\circ$  a separation that remains constant over this frequency range. It is worth noticing that both the PC and the IP are  $\approx 80\%$  weaker than the MP and are located almost symmetrically around the profile midpoint. Whether low-level emission connects each one of these components to the MP is of great importance in interpreting this profile as single-pole or double-pole emission. Further data with higher signal-to-noise are required to settle this issue.

The relative strength and separation of the PC and IP appear to be frequency independent. At the same time, the MP shows a significant change in shape between 430 MHz and 1.4 GHz, with its trailing part (component A) becoming progressively weaker. Core components tend to weaken with frequency, allowing for a pair of outriders around them to emerge. However, the MP of this profile exhibits only one conal outrider (component B) making doubtful the association of component A with a core component hence the profile development *abnormal*. The MP of J2019+2425 could be a so-called partial cone, where only one of the two conal outriders is present. Partial cones are a relatively rare phenomenon, to date seen only amongst normal pulsars (Lyne & Manchester 1988). However, the presence of two additional components which are symmetrically spaced around the MP makes this interpretation difficult, at least if the dominant field is a dipole. Polarimetric data of high quality are required to shed light into the interpretation of this profile.

### 3.22. PSR J2051–0827

This pulsar is a member of a binary system with an extremely low mass companion ( $\approx 0.03M_{\odot}$ ) in a tight circular orbit which eclipses the pulsar at radio frequencies below  $\approx 1$  GHz (Stappers *et al.* 1996). It exhibits a simple profile that resembles those of core single pulsars, with a moderate degree of linear and circular polarization that preserves one sense throughout the profile. The low-level linear polarization seen here could be associated with the presence of more components in this seemingly simple profile (cf. paper I).

### 3.23. PSR J2145–0750

This MSP (Bailes *et al.* 1994) is orbited by a  $\approx 0.51M_{\odot}$  white-dwarf companion in a wide circular orbit, which has been identified optically at the timing position of the pulsar (Bell *et al.* 1995). This pulsar exhibits a complex pulse morphology and complicated polarization properties. The profile consists of a main pulse which closely resembles that of PSR B1237+25. However, it also exhibits a precursor. The precursor of the Crab pulsar is separated from its MP by some  $21^{\circ}$  while a bridge of low-level emission appears to connect the two features. The post-cursor of another normal pulsar, PSR B0823+26, is separated from its MP by about  $30^{\circ}$ , again with low-level emission connecting the two features. In contrast, the precursor of PSR J2145–0750 is located relatively far away ( $\approx 96^{\circ}$ ) from the centre of the MP and it is an unusual feature to interpret. At 1.4 GHz, we see no low-level emission connecting the MP to the precursor. We note that the precursor is not always detectable in our shorter sub-integrations, as far as can be inferred from the given signal-to-noise ratio. At very low frequencies (102 MHz), the precursor is not detected at all (Kuzmin & Losovsky 1996), while the separation of the precursor peak to the leading edge of the MP remains unchanged between 430 MHz (Lorimer 1994), 800 MHz ( Backer 1995), and 1.4 and 1.7 GHz (this paper and paper I), suggesting emission from a single pole. Under the sharp leading component, the strange signature of both the linear and circular polarization does not suggest any

firm profile classification. The PPA curve deviates significantly from an RVM curve, and is rather flat. Moreover, there is no indication in the linear polarization that orthogonal mode-changing activity is present which could alter the shape of the PPA curve. Therefore, the PPA curve of this pulsar is hard to reconcile with a RVM curve, even if disturbed by mode-changing activity. The existence of a precursor at an unexpected location, together with the severely perturbed PPA curve, gives strong evidence for distortion of the magnetic field in the emission regions of this source.

### 3.24. PSR J2229+2643

This pulsar is a member of a binary system in a wide circular orbit with a  $\approx 0.26M_{\odot}$  companion. It exhibits the weakest inferred surface magnetic dipole field strength in any known pulsar. The 430-MHz profile (Camilo *et al.* 1996b) has *not evolved* by 1.4 GHz, and profile narrowing with frequency is not seen. The PPA is shallow, and high linear and moderate circular polarization is evident.

### 3.25. PSR J2317+1439

PSR J2317+1439 is orbiting a  $\approx 0.21M_{\odot}$  companion in a wide circular orbit (Camilo *et al.* 1996b). The multiple-component profile structure seen at 430 MHz indicates that the bright feature at the central part of the profile is the core component. Indeed, at 1.4 GHz this component has faded and become equal in intensity with the leading component, *as expected* for a multiple-component profile. There is significant circular polarization within the central part of the profile, while the linear polarization remains at moderate levels. The PPA curve exhibits a  $90^{\circ}$  discontinuity associated with a drop of linearly polarized intensity. There is no significant narrowing of the profile width between 1.4 and 1.7 GHz.

### 3.26. PSR J2322+2057

PSR J2322+2057 is an isolated pulsar. Its relatively narrow, simple components appear moderately polarized. The  $\Delta\phi_{\text{MP-IP}} = 234^{\circ}$  separation, remains unchanged with frequency to the extent that it can be traced from the 430-MHz profile (Nice *et al.* 1993). As with PSR B1855+09 (Kijak *et al.* 1997), PSR J2322+2057 shows a decreasing MP-IP intensity ratio with increasing frequency *in contrast* to the general trend seen in the MP-IP development for normal pulsars. The components are simple, but much narrower than expected if a simple dipolar field structure is assumed to prevail in the radio-emission region.



#### 4. Contrasting MSP and normal pulsar polarization properties

It is evident from the discussion of Section 3, that the frequency development of the profiles and the associated polarization characteristics do not point towards a clear classification for most of the MSPs studied. Instead, we have identified pulsars for which spectral profile development can be described as *normal* (**N**), *minimal* (**M**) or *abnormal* (**A**). This profile evolution is assigned to each source in Table 2 (col. 9), which also lists the physical parameters that may regulate the radio emission of each source. A *minimal* development characterizes profiles which exhibit virtually no change between frequencies of 400 MHz and 1.4 GHz. We characterize profiles as *normal* those which develop according to the scheme of Rankin (1983a;b). Finally, *abnormal* development characterizes profiles which are inconsistent with the predictions of Rankin’s classification scheme. The failure of the classification scheme to account for the emission properties seen in MSPs could be attributed to either a change in the emission mechanism itself for these much shorter rotational periods, or to modifications in the local environment, namely the magnetic-field structure in the emission region.

A quantitative comparison is presented in this section between the emission properties of millisecond and normal pulsars. The polarization parameters for the pulsars discussed above are summarized in Table 1. The mean linear (col. 2) and circular (cols. 3 and 4) polarization represent the ratio of the area under the  $L$  or  $|V|$  (and  $V$ ) curve respectively to the area under the  $I$  curve shown for each pulsar in Figs. 1-6. The maximum fitted slope of the PPA curve  $\left(\frac{d\psi}{d\phi}\right)_{\max}$ , is given in col. 5, whenever its determination was possible. The values listed in Table 1 are used to make a quantitative comparison between the distribution of 1.4 GHz polarization parameters for normal and MSPs. In Fig. 7a, we present the histogram of the 1.4 GHz fractional linear polarization for 281 normal pulsars from the sample of Gould (1994) and for our measurements of 24 MSPs. This sample includes the polarization of two MSPs with IPs. It is evident that the fractional linear polarization is higher on average at 1.4 GHz for MSPs (Fig. 7a, upper panel) than for normal objects (Fig. 7a, lower panel). A similar effect is observed in the absolute value of the circular polarization (Fig. 7b) with MSPs having statistically significant higher polarizations than normal pulsars. The histogram of the values of circular polarization is presented in Fig. 7c where the sense of circularity has been determined in our sample by referencing our measurements to PSR B1929+10 whenever this was possible. The deviation of the peak of this histogram from zero is at  $2\sigma$  of its mean value. This could be attributed to a systematic instrumental effect but also suggests that the distribution presented is incomplete.

The difference in the degree of polarization is further established by the results of a Kolmogorov-Smirnov test that indicates a very low probability (0.0004%) that the two populations are similarly polarized either in the linear or the circular component. Our sample includes half of the known MSPs with periods shorter than 30 ms, and the results presented in Figs. 7a-c might change as more MSPs are studied polarimetrically. However, from this data set, evidence is presented that MSP emission is more polarized than that of normal pulsars at 1.4 GHz.

Another result comes from comparing the distribution of the slopes of the PPA curves for MSPs

with that for normal pulsars in the Lyne & Manchester (1988) sample (Fig. 7d). Even though some of our observations (PSRs J1643–1224, B1744–24A and B1953+29) have been influenced by dispersion smearing, we note that MSPs in general have much shallower slopes than normal pulsars. A Kolmogorov-Smirnov test shows that the two distributions differ significantly. A similar comparison was also made with groups of normal pulsars which were sorted according to their profile class. Our result is independent of profile class. It is evident from the polarization profiles (Figs. 1-6) that the PPA curves of most MSPs, (a) cannot be easily described by a RVM curve, (b) exhibit rather small excursions, and (c) possess shallow slopes.

The polarization state of pulsar radio emission in a canonical pulsar model is regulated by one or both of the following : (i) propagation effects, and (ii) a geometrical overlapping of the elementary beams of emission. Deviations from the canonical model in MSP magnetospheres might result in additional effects, modifying in some fashion the polarization state (e.g. Chen & Ruderman 1993b).

One class of models of radio pulsar magnetospheres predicts an outflowing electron-positron plasma through which radio-waves propagate. Propagation effects through this plasma should have several observational consequences, as demonstrated by Cheng & Ruderman (1980) and extensively studied by Shitov (1985) and Barnard (1986). The propagation modes maintain a nearly fixed phase relationship, and thus a constant polarization state at a certain *limiting* radius. Barnard (1986) showed that under certain physical conditions (depending on the rotational period  $P$  and the magnetic field strength  $B$ ), this limiting radius approaches the light cylinder radius ( $R_{LC}$ ) so that the field lines become quite swept-back, exhibiting an increasingly azimuthal component. In this case, the familiar S-shaped PPA curve will be modified (Barnard 1986, Fig. 1). The PPA will typically undergo a smaller swing and its curve will exhibit a shallower slope due to the uniformity of the magnetic field as a result of the azimuthal component contribution. The small excursions in the PPA curves seen in the MSP profiles, together with their shallower slopes make these models a possible interpretation if indeed emission from close to the light cylinder is an option. Furthermore, emission at  $R_{LC}$  would imply morphological asymmetries in the integrated profiles.

Alternatively, geometric arguments (Morris *et al.* 1981; Xilouris *et al.* 1995) relate the polarization state of the radio emission to the size of pulsar magnetospheres, assuming processes such as curvature radiation to be responsible for pulsar emission. Significant fractional polarization evident in short-period pulsars is consistent with the canonical pulsar model, in which relativistic charges flow along dipolar field lines and emit curvature radiation beamed tangentially to the field lines into narrow cones of opening angle  $1/\gamma$ , where  $\gamma$  is the relativistic Lorentz factor. The dipolar field lines, which control the motion of the charged particles, diverge more for short-period pulsars at a given radius than for long-period pulsars. Assuming that the elementary beams of emission are period independent, they would then overlap less. This could therefore lead to a high degree of linear polarization. In contrast, converging beams would lead to depolarization of the instantaneous radiation (see also Gil & Snakowski 1990). While this geometric interpretation could account for the somewhat higher fractional polarization seen in MSPs, it would require a special geometry for the magnetic field in order to account for disturbed PPA curves exhibiting shallow excursions and

flat slopes.

Special field geometries could, for instance, emerge from modified polar cap regions, such as those described by Chen & Ruderman (1993b). In the case of PSR B1937+21 they showed that the distorted magnetic field would heavily influence the fractional linear polarization and at the same time flatten out the PPA curve. While a firm identification of the core component in most of our MSP profiles is rare, we point out that for these few cases the profiles preserve a symmetry in their morphology. In the presence of special field geometries, surface emission models would result in complicated and rather asymmetric profiles. Such asymmetries are not evident in the profile of PSR 1937+21 for instance.

The processes that regulate the degree of polarization, either geometrical in origin or the result of propagation effects at the light cylinder, do depend on the rotational period. However, the magnetospheric phenomena known to characterize the emission of normal pulsars, such as orthogonal polarization modes, sense-reversing circular polarization, or even intensity and polarization mode-changing and intensity fluctuations, are clearly evident in the MSP polarimetric profiles. This strongly suggests that the basic properties of the emission mechanism have not been influenced by the change in rotational period. Some unusual properties which we have identified in the previous section could therefore be attributed to environmental changes in the emission regions. Such changes could be, (a) special geometries due to mass accretion (e.g. Chen & Ruderman 1993b) or higher order magnetic field multipoles near the stellar surface (e.g. Manchester & Johnston 1995), or (b) migration of the location of the emission regions closer to the  $R_{LC}$  (e.g. Barnard 1986). A study of the frequency dependence of the polarization properties of MSPs is eagerly awaited to clarify these issues.

## 5. The impact of the magnetic field on millisecond pulsar emission.

So far we have shown that millisecond and normal pulsars most likely share the same emission process, however, some MSPs exhibit unusual properties which are not easily understood in the frame of a canonical pulsar model. Certain physical parameters have been considered by various magnetospheric models as factors that condition the emission. Some of these parameters are given in Table 2 for the pulsars in our sample. In this section we investigate their role in the regulation of the emission process. At the same time we search for common properties among the diversity exhibited by MSPs, establishing in this way groups that may form the basis of future MSP classification schemes.

The distribution of  $P$  (Table 2, col. 2) of MSPs exhibiting abnormal profile development is relatively narrow, having an average value of 4.5 ms. In contrast, MSPs which exhibit normal characteristics populate a much broader range as can also be seen in Fig. 8c. The dipole component of the surface magnetic field ( $B_0$ ) can be estimated using the  $P$  and  $\dot{P}$  of each pulsar. The values of  $\dot{P}$ , corrected for kinematic effects (cf. Camilo *et al.* 1994b) are used to estimate a lower limit

( $\alpha = 90^\circ$ ) of the dipole component given in Table 2 (col. 3). We note that pulsars exhibiting abnormal profile behavior are associated with low values of  $B_0$ . The respective distribution of MSPs with normal characteristics is quite broad, while on average they tend to exhibit higher fields.

A threshold parameter for the pulsar phenomenon is the potential drop ( $\Delta V$ ) across the polar cap (e.g. Sturrock 1971), given by  $\Delta V \approx B_{12}/P^2$  (Table 2, col. 4). This parameter also constraints the size of sparks generated above a homogeneously illuminated polar cap (Ruderman & Sutherland 1975; Cheng & Ruderman 1980). A great scatter is evident among the values of  $\Delta V$  for the three classes of MSPs that we have identified (Fig. 8a). However, we note that most of them, particularly those with abnormal profile development (marked with filled circles on Fig. 8a) exhibit relatively high values of the accelerating potential. High values of  $\Delta V$  are representative of normal pulsars classified as core-single (Rankin 1993b), where  $\Delta V$  is 2.5 on the average. Core-single stars are typically young normal pulsars with narrow beams. If indeed  $\Delta V$  regulates in some fashion the radio emission then the abnormal properties of MSPs might be encountered among the very young normal pulsars.

Beskin *et al.* (1988) proposed the parameter  $Q \approx 2P^{11/10}\dot{P}_{15}^{-4/10}$ , to distinguish between the propagation modes in pulsar magnetospheres. Values of  $Q < 1$  represent extraordinary propagation modes while  $Q > 1$  are associated with normal propagation modes of radiation. According to the classification of some 150 pulsars (Rankin 1993b), values of the propagation parameter  $1/Q > 1$  are associated with the younger pulsars among the normal-pulsar population. Similar values seem to be representative of the MSPs in our sample (see col. 5 of Table 2), suggesting common properties of the polarization between the two groups. Indeed, core-single profiles are associated with moderate degree of linear and significant circular polarization. If the conditions in MSP magnetospheres favour the presence of extraordinary modes, then the high degree of circular polarization often identified in MSP emission, might be the net result of the propagation of such modes.

The MSP magnetospheres are radially compact as can be seen from the values of the light cylinder radii ( $R_{LC}$ ), given in col. 6 of Table 2. This suggests that any frequency stratification in their magnetospheres (radius-to-frequency mapping; e.g. Cordes 1978) should be hardly evident in the pulse widths if we assume that the magnetic field has preserved its dipole structure within the emission region. MSPs exhibiting abnormal profile development in our sample tend to exhibit the most compact magnetospheres with an average radius of  $R_{LC} \approx 200$  km. They are also associated with wide polar caps (see Table 2, col. 7). Possibly, some of the abnormal effects evident in MSP profiles might be related to higher order multipoles acting in very radially compact but azimuthally extended magnetospheres. In contrast, sources in our sample that exhibit minimal or normal profile development possess somewhat larger magnetospheres though still compact if compared with normal pulsars. The frequency dependence of the pulse widths of these MSPs suggests a very minimal radius-to-frequency mapping in their magnetospheres, if at all. This implies that the presence of higher order multipoles is rather limited. Indeed, a radius-to-frequency mapping acting in the presence of higher order fields would result in more prominent profile changes than

those observed. However, it is also possible that radius-to-frequency mapping scales in some fashion with  $P$ . Multifrequency studies are needed to explore the period dependence of radius-to-frequency mapping in MSPs.

Modifications are expected in MSP polar caps and hence the magnetic field topology as a result of the accretion during the mass transfer stage of their evolution (e.g. Ruderman 1991; Chen & Ruderman 1993b). Most likely this modification is regulated by the total mass transferred and the duration of this process, while the initial rotational period at the beginning of mass transfer might also act as a tuning factor. We note that the companion mass of MSPs with abnormal properties in our sample is less than  $0.4M_{\odot}$  (col. 8). This associates them primarily with low mass companions, mostly Helium white dwarfs. In contrast, MSPs classified as normal or minimal, are orbited both by Helium and Carbon-Oxygen companions. High-mass binary pulsars are expected to have accreted a smaller amount of mass than low-mass systems. The preference of MSPs with abnormal emission properties to be in low-mass systems suggests that these stars might be associated with substantial mass transfer and very short final rotational periods. In paper I, a weak anti-correlation was found between profile development and companion mass as well as rotational period. Here we see that MSPs exhibiting abnormal profile development are associated with substantial mass transfer and a narrow range of periods.

We have computed the magnetic field at the light cylinder ( $B_{LC}$ ) for all known MSPs, assuming a purely dipolar magnetosphere. This is shown in Fig. 8b, as a function of period. In Fig. 8b as well as in Figs. 8c and 8d, MSPs with abnormal profile properties are identified by filled symbols. Pulsars with IPs (PSRs J1012+5307, B1534+12, J1730–2304, J1744–1134, B1821–24, B1855+09, B1937+21, B1957+20, J2019+2425, J2317+1439 and J2322+2057) as well as pulsars with components on their baselines (pre- and post-cursors, i.e. PSRs J1518+4904, J1730–2304, J1744–1134, B1953+29, B1957+20, J2019+2425, J2145–0750 and J2317+1439) are marked with triangles pointing up. Pulsars with extended emission over their period or low-level emission at a wide range of longitudes are shown as triangles pointing down (PSRs J0218+4232, J0437–4715, J0751+1807, J1012+5307, B1534+12, B1855+09, B1957+20, J2019+2425 and J2317+1439). For comparison we also present the Crab (marked with a diamond) and the Vela pulsar (marked with a square). We note that very few sources maintain a relatively high magnetic field strength ( $10^6$  G) at their light cylinder (Fig. 8b) which is similar to that of the Crab pulsar. Among these sources are PSRs J0034–0534, J0218+4232, B1937+21 and B1957+20. The IP of B1957+20 exhibits the most abnormal profile development seen among MSPs while its MP as well as the components of PSR B1937+21 are unusually narrow features. Like the Crab pulsar, B1937+21 exhibits unusual single pulses (Cognard *et al.* 1996). Although the majority of MSPs maintains low magnetic fields near their light cylinders, many MSPs possess magnetic fields as found for the Vela pulsar (i.e.  $10^4$  –  $10^5$  G) and simultaneously exhibit an abnormal profile development. In addition, we note that pulsars with IPs tend to form a boundary line, implying a period dependence of the existence of IPs on  $\dot{P}$ . Pulsars with extended emission also cluster along this boundary line. Some magnetospheric models imply that the magnetic field at the emission region of normal pulsars lies in the range  $10^6$

-  $10^7$  G (e.g. Ruderman & Sutherland 1975). This condition is satisfied at the vicinity of the light cylinder by very few MSPs. MSPs with abnormal profile development as well as those with IPs or components of emission on their baselines, satisfy this condition at a somewhat lower emission height which however corresponds still to a significant fraction of their light cylinder. Indeed, if a field of  $10^6$  G is essential for the creation of radio emission, some MSPs could be potential outer gap emitters. However, MSPs with unusually narrow components (e.g. B1937+21), presumably due to some current re-distribution, might meet this condition elsewhere in their magnetospheres. Finally, there might be hybrid cases (e.g. B1957+20) where emission from outer gaps as well as traditional polar cap emission might co-exist.

The distribution of MSPs on the  $P - \dot{P}$  diagram has been attributed to spin-up during disk accretion, if these stars have dipolar magnetospheres. In Fig. 8c, we present the  $P - \dot{P}$  diagram for all known MSPs. Superimposed on this are the spin-up lines for dipole and quadrupole magnetospheres as calculated by Arons (1993). Fig. 8c shows that, at the present stage of their evolution, some of the MSPs are located near the dipolar spin-up line. However, there is a substantial number of sources which presumably do not share the same age or evolution, that cluster around the quadrupole spin-up line. This spin-up line is calculated assuming that a quadrupole field dominates the magnetosphere. We note that abnormal MSPs are clustering around this spin-up line. If indeed these stars are associated with complicated fields dominating their magnetospheres, they might exhibit a somewhat higher value of the braking index.

While polar-cap models (e.g. Ruderman & Sutherland 1975) require strong fields to sustain pair production, another series of models, which involve emission from outer-gaps (e.g. Cheng *et al.* 1986) require somewhat reduced field strength. Indeed, outer-gap emission is strongly dependent on the magnetic-field strength, as seen from Fig. 8d where the surface dipole fields of all known MSPs are plotted against  $P$ . According to the model of Chen & Ruderman (1993a), this diagram is separated into one region where the traditional polar-cap emission prevails (region III), and two regions where emission from outer gaps is possible (regions I and II). Region II includes pulsars which share common emission properties with the Vela pulsar, while the properties that correspond to pulsars populating region I are similar to the Crab pulsar. The death-line separating regions II and III corresponds to the maximum of  $\gamma$ -ray emission which, according to some authors, can occur only from the outer magnetospheric gaps. However, we should note that these lines are strongly dependent on the assumed magnetic field structure (e.g. Phinney & Kulkarni 1994). We note that pulsars with IPs and extended emission, populate the border line that separates traditional polar-cap from outer-gap emission. According to a model by Romani & Yadigaroglu (1995), there is a variety of combinations of  $\alpha$  and  $\beta$  that would allow the detection of this type of emission. The highest probability exists when an orthogonal rotator ( $\alpha = 90^\circ$ ) is viewed. Our observation that most of the sources that fall on the border-line are pulsars with IPs or exhibit extended emission, is in good agreement with the predictions of this model. This suggests that a significant percentage of MSPs which combine IPs with extended baseline emission could be understood as outer-gap emitters. However, pulsars such as B1937+21 exhibit IPs, lacking any observationally confirmed

low-level emission. In addition, a simple scaling of the canonical pulsar model fails to describe the narrow beams of the MP and IP of this source (paper I). This pulsar is then better understood if the prevailing emission still originates from a traditional polar cap which is not bound by the last open field lines, but is rather contracted in size, forced by some kind of redistribution of currents. Such a modification could be the product of the accretion process responsible for the rebirth of this source (Chen & Ruderman 1993b). However, it could also have its origins on a pure geometrical contraction of the emission region, necessary for its accommodation within the minute light cylinder of this pulsar at regions where conditions favour radio emission. Conceivably, this contraction could account for the systematically narrower emission beams evident in other MSPs as has been demonstrated in paper I.

## 6. Conclusions

To date, systematic surveys have revealed more than 40 pulsars with periods  $\leq 30$  ms (Camilo 1997). The emission properties of a sizable number of these sources have been monitored for a period of three years at a frequency of  $\lambda 21$  cm with the Effelsberg 100-m radio telescope. Our conclusions are presented in a series of papers. In paper I, we presented the spectra and luminosities of MSPs and investigated the profile complexity and the beam shape. Millisecond pulsars are slightly less luminous sources, while their spectra are identical to those of normal pulsars. We have shown that the complexity in MSP profiles is comparable to that seen in normal pulsars. Their beam size does not follow the scaling predicted by a canonical pulsar model. Rather, a critical period exists below which the beams of MSPs appear narrower than expected.

In this work we have shown that the frequency development of the polarization profiles and their properties do not comply with the predictions of the classification schemes developed for normal pulsars. Instead, we can identify three classes of profiles: (a) those that evolve minimally (M); (b) those that evolve as predicted (N); and (c) those that evolve contrary to any prediction (A). Eight pulsars in our sample exhibit abnormal profile development and are associated with short periods, low surface magnetic fields and compact magnetospheres which could possibly engulf strong higher multipole moments. In contrast, pulsars that evolve minimally or even normally, are associated with somewhat larger and possibly dipolar magnetospheres. A very slow radius-to-frequency mapping must persist in their magnetospheres, and is responsible for the minimal profile change with frequency.

We find evidence that MSP emission is more polarized than that of normal pulsars. Moreover, the PPA curves of most MSPs, (a) cannot be easily described by a RVM curve, (b) exhibit rather small excursions, and (c) possess flat slopes. These properties make models that support emission from locations that constitute a substantial fraction of the light cylinder (e.g. Barnard 1986) a possible interpretation. However, special geometries resulting from the binary nature of the sources (e.g. Chen & Ruderman 1993b), or higher multipole moments (e.g. Manchester & Johnston 1995), could influence the polarization characteristics in a similar manner, prohibiting a clear

interpretation of the data, at least from the current single-frequency observations.

Pulsars like B1937+21 and B1957+20 have beams which are narrower than a simple scaling down of normal pulsar magnetospheres. This discrepancy can be reconciled if the emission in some MSPs still originates from a traditional polar cap, but is not bound by the last open field lines. A possible redistribution of currents, either as the result of an evolutionary effect or due to some scaling imposed by  $P$  and  $\dot{P}$ , could force the emission beam to become azimuthally narrow. This scenario could account for the narrow pulses of B1937+21 and the MP of B1957+20. However, the MP of B1957+20 exhibits different properties that are better understood if its emission originates from the vicinity of the light cylinder. The profile asymmetries as well as the extra components of emission on the baseline can be understood in this model, as the net effect of field lines swept-back in the azimuthal direction.

Evidently, the strength and topology of the magnetic field play an important role in regulating the emission in MSP magnetospheres. Some sources maintain a strong dipolar field ( $10^6$  G) at locations which constitute a significant fraction of their light cylinder. Among those, some pulsars with IPs and extended emission can be found. Pulsars with abnormal profile development also seem to radiate from such locations.

Although the fashion in which the presence of higher multipole moments influences the profile shape and the polarization characteristics is uncertain, we note that pulsars with IPs that show abnormal properties cluster around the quadrupolar spin-up line in the  $P - \dot{P}$  diagram. If indeed the magnetospheres of these stars are quadrupolar this implies that they might exhibit a higher than the average braking index.

The combination of  $B_0$  and  $P$  of some pulsars with IPs and extended emission places these sources near the death-line that separates outer-gap emission from traditional polar-cap emission. According to certain models (e.g. Romani & Yadigaroglu 1995), the highest probability of detecting emission from outer magnetospheric gaps exists for an orthogonal rotator. This prediction is in very good agreement with our findings, suggesting that the low-level emission and the unusual features identified in the baselines of some MSPs could result from outer gaps. However, not all pulsars with IPs fit in this scheme since extended emission at low-levels is not identified (e.g B1937+21), nor are all pulsars with IPs abnormal in their frequency evolution. Depending on certain physical or geometrical parameters and possibly below a critical rotational period, the emission region could have migrated into locations where more favourable conditions exist.

Millisecond pulsar magnetospheres are indeed compact and the distinction between inner and outer magnetospheric regions might not be as clear as in the case of normal pulsars. It could be that the emission is regulated by a combination of processes where favourable conditions decide on the prevailing process. The work presented in this paper represents first attempt to understand the emission of MSPs based on a large sample of objects. Multi-frequency polarimetric and timing observations are essential in shedding light on the issue of the location of the emission region and the structure of the magnetic field in MSP magnetosphere.



We are thankful to C. Salter, J. Eder and Z. Arzoumanian for their helpful comments. We are also grateful to the unknown referee for his helpful comments. FC gratefully acknowledges the support of the European Commission through a Marie Curie fellowship, under contract nr. ERBFMBICT961700. This work was in part supported by the European Commission under the HCM Network Contract nr. ERB CHRX CT960633, i.e. the *European Pulsar Network*. Arecibo Observatory is operated by Cornell University under cooperative agreement with the National Science Foundation.

## REFERENCES

- Arons, J. 1993, ApJ, 408, 160
- Arzoumanian, Z., Phillips, J. A., Taylor, J. H., & Wolszczan, A. 1996, ApJ, 470, 1111
- Ashworth, M., Lyne, A. G., & Smith, F. G. 1983, Nature, 301, 313
- Backer, D. C. 1995, JAA, 16, 165
- Backer, D. C., Foster, R. F., & Sallmen, S. 1993, Nature, 365, 817
- Bailes, M., et al. 1994, ApJ, 425, L41
- Bailes, M., et al. 1997, ApJ, 481, 386
- Barnard, J. J. 1986, ApJ, 303, 280
- Becker, W., Trümper, J., Lundgren, S. C., Cordes, J. M., & Zepka, A. F. 1996, MNRAS, 282, L33
- Bell, J. F., Kulkarni, S. R., Bailes, M., Leitch, E. M., & Lyne, A. G. 1995, ApJ, 452, L121
- Bell, J. F., Bailes, M., Manchester, R. N., Lyne, A. G., Camilo, F., & Sandhu, J. S. 1997 MNRAS, 286, 463
- Beskin, V. S., Gurevich, A. V., & Istomin, Y. N. 1988, Sov. Astron. Lett., 14, 93
- Bhattacharya, D. 1992, in Proc. of IAU Colloq. 128, ed. T. Hankins, J.M. Rankin, J. A. Gil, (Zielona Gora: Pedagogical University Press), p. 27
- Boriakoff, V., Buccheri, R., & Fauci, F. 1986, Nature, 304, 417
- Camilo, F. 1995, Ph.D thesis, Princeton University
- Camilo, F. 1997, in: High Sensitivity Radio Astronomy, eds. N. Jackson and R. J. Davis, (Cambridge: Cambridge University Press), p. 14
- Camilo, F., Foster, R. S., & Wolszczan, A. 1994a, ApJ, 437, L39

- Camilo, F., Thorsett, S. E., & Kulkarni, S. R. 1994b, *ApJ*, 421, L15
- Camilo, F., Nice, D. J., Shrauner, J. A., & Taylor, J. H. 1996a, *ApJ*, 469, 819
- Camilo, F., Nice, D. J., & Taylor, J. H. 1996b, *ApJ*, 461, 812
- Camilo, F., Kramer, M., Nice, D.J., Xilouris, K.M., Taylor, J.H., & Shrauner, J.A. 1998, in preparation
- Chen, K., & Ruderman, M. A. 1993a, *ApJ*, 402, 264
- Chen, K., & Ruderman, M. A. 1993b, *ApJ*, 408, 179
- Cheng, A. F., & Ruderman, M. A. 1980, *ApJ*, 235, 576
- Cheng, K. S., Ho, C., & Ruderman, M. A. 1986, *ApJ*, 300, 522
- Cognard, I., Shrauner, J. A., Taylor, J. H., & Thorsett, S. E. 1996, *ApJ*, 457, L81
- Cordes, J. M. 1978, *ApJ*, 222, 1006
- Cordes, J. M., & Stinebring, D. R. 1984, *ApJ*, 277, L53
- Damour, T., & Taylor, J.H. 1992, *Phys. Rev. D*, 45, 1840
- Foster, R. S., Fairhead, L., & Backer, D. C. 1991, *ApJ*, 378, 687
- Foster, R. S., Wolszczan, A., & Camilo, F. 1993, *ApJ*, 410, L91
- Foster, R. S., Cadwell, B. J., Wolszczan, A., & Anderson, S. B. 1995, *ApJ*, 454, 826
- Fruchter, A. S., Berman, G., Bower, G., Convery, M., & Goss, W.M. 1990, *ApJ*, 351, 642
- Gil, J. A. 1983, *A&A*, 127, 267
- Gil, J. A., & Snakowski, J. K. 1990, *A&A*, 234, 269
- Gould, D. M. 1994, Ph.D thesis, University of Manchester
- Hankins, T. H., & Fowler L. A. 1986, *ApJ*, 304, 256
- von Hoensbroech, A., & Xilouris, K. M. 1997, *A&A*, 324, 846
- van Kerkwijk, M. H., Bergeron, P., & Kulkarni, S. 1996, *ApJ*, 467, L89
- Kijak, J., Kramer, M., & Wielebinski, R. 1997, *A&A*, 318, L63
- Kramer, M., Xilouris, K. M., Lorimer, D. R., Jessner, A., Wielebinski, R., Wolszczan, A., Camilo, F. 1997, *ApJ*, in press (paper I)

- Kramer, M., Xilouris, K. M., Camilo, F., Doroshenko, O., Nice, D. J., Jessner, A., 1998, in preparation (paper IV)
- Krolik, J. H. 1991, *ApJ*, 373, L69
- Kuzmin, A. D., & Losovsky, B. Ya. 1996, *A&A*, 308, 91
- Lorimer, D. R. 1994, Ph.D thesis, University of Manchester
- Lorimer, D. R., et al. 1995a, *ApJ*, 439, 933
- Lorimer, D. R., Lyne, A. G., Festin, L., & Nicastro, L., 1995b, *Nature*, 376, 393
- Lundgren, S. C., Zepka, A. F., & Cordes, J. M. 1995, *ApJ*, 453, 419
- Lyne, A. G., & Manchester, R. N. 1988, *MNRAS*, 234, 477
- Lyne, A. G., Biggs, J. D., Brinklow, A., Ashworth, M., & McKenna, J. 1988, *Nature*, 332, 45
- Lyne, A. G., et al., 1990, *Nature*, 347, 650
- Manchester, R. N. 1992, in *Proc. of IAU Colloq. 128*, ed. T. Hankins, J.M. Rankin, J. A. Gil, (Zielona Gora: Pedagogical University Press), p. 206
- Manchester, R. N., & Johnston, S. 1995, *ApJ*, 441, L65
- McKinnon, M. M. 1993, *ApJ*, 413, 317
- Morris, D., Graham, D. A., & Sieber, W. 1981 *A&A*, 100, 107
- Navarro, J., & Manchester, R. N. 1996, in *Proc. IAU Colloq. 160, Pulsars: Problems & Progress*, ed. S. Johnston, M. Walker, M. Bailes, (San Francisco: PASP), p. 249
- Nicastro, L., Lyne, A. G., Lorimer, D. R., Harrison, P. A., Bailes, M., & Skidmore, B. D. 1995, *MNRAS*, 273, L68
- Nice, D.J. 1992, Ph.D thesis, Princeton University
- Nice, D. J., Taylor, J. H., & Fruchter, A. S. 1993, *ApJ*, 402, L49
- Nice, D. J., Sayer, R. W., & Taylor, J. H. 1996, *ApJ*, 466, L87
- Pechenick, K. R., Ftaclas, C., Cohen, J. M. 1983, *ApJ*, 274, 846
- Phinney, E. S. & Kulkarni, S. R. 1994, *ARA&A*, 32, 591
- Radhakrishnan, V., & Cooke, D. J. 1969, *Astrophys. Lett.*, 3, 225
- Rankin, J. M. 1983a, *ApJ*, 274, 333

- Rankin, J. M. 1983b, *ApJ*, 274, 359
- Rankin, J. M. 1990a, *ApJ*, 352, 247
- Rankin, J. M. 1992b, in *Proc. of IAU Colloq. 128*, ed. T. Hankins, J.M. Rankin, J. A. Gil, (Zielona Gora: Pedagogical University Press), p. 133
- Rankin, J. M. 1993a, *ApJ*, 405, 285
- Rankin, J. M. 1993b, *ApJS*, 85, 145
- Romani, R. W., & Yadigaroglu, I. A. 1995, *ApJ*, 438, 314
- Ruderman, M. A. 1991, *ApJ*, 382, 576
- Ruderman, M. A. & Sutherland P. G. 1975, *ApJ*, 196, 51
- Ryba, M. F., & Taylor, J. H. 1991, *ApJ*, 371, 739
- Segelstein, D. J., Rawley, L. A., Stinebring, D. R., Fruchter, A. S., & Taylor, J. H. 1986, *Nature*, 322, 714
- Shitov, Y. P. 1985, *Soviet Astr.*, 29, 33
- Stappers, B. W., et al. 1996, *ApJ*, 465, L119
- Stinebring, D. R., & Cordes, J. M. 1983, *Nature*, 306, 349
- Stinebring, D. R., Cordes, J. M., Weisberg, J. M., Rankin, J. M., & Boriakoff, V. 1984, *ApJS*, 55, 247
- Sturrock, P.A. 1971, *ApJ*, 164, 529
- Thorsett, S. E., & Stinebring, D. R. 1990, *ApJ*, 361, 644
- Thorsett, S. E., Fruchter, A. S., Stinebring, D. R. & Taylor, J. H. 1989, in *Proc. 14th Texas Symposium on Relativistic Astrophysics*, ed. E. J. Fenyves, (New York: New York Academy of Sciences), p. 420
- Wolszczan, A., & Frail, D. A. 1992 *Nature*, 355, 145
- Xilouris, K. M., Seiradakis, J. H., Gil, J. A., Sieber, W., & Wielebinski, R. 1995, *A&A*293, 153
- Xilouris, K. M., Kramer K., & von Hoensbroech, A. 1998a, in preparation (paper III)
- Xilouris, K.M., et al. 1998b, in preparation

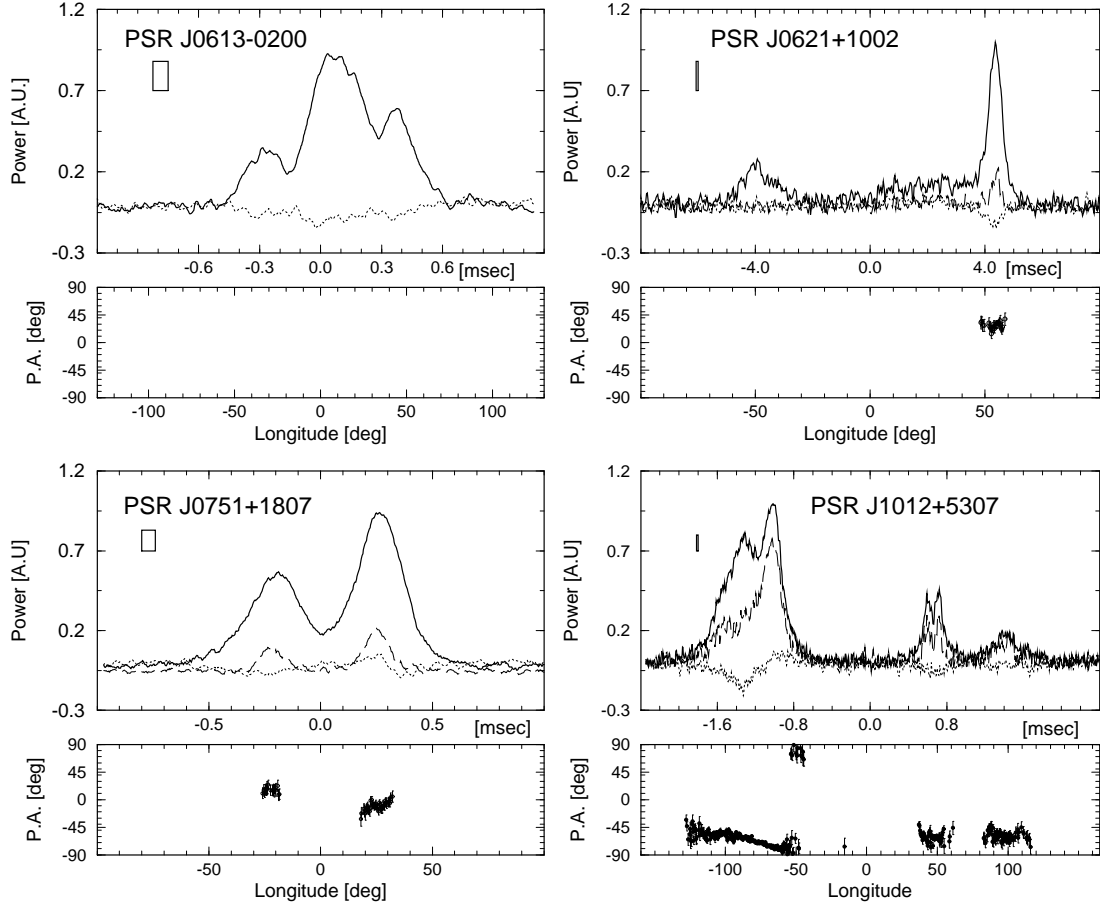


Fig. 1.— 1410 MHz polarization profiles of 23 MSPs. Four curves are plotted: the total power (Stokes parameter  $I$ ) is the outer curve, whose maximum is scaled to arbitrary units. The linear polarization (Stokes  $L = (Q^2 + U^2)^{1/2}$ ) is the interior, dashed curve, and the circular polarization (Stokes  $V = \text{LCP} - \text{RCP}$ ) is the dotted curve. The linear PPA curve is plotted on the lower panel in degrees and measured counter-clockwise from north on the plane of the sky. The PPA curve is plotted only when the linear polarization is greater than  $2\sigma$ , except in the cases of PSRs J0613-0200, B1534+12 and J2322+2057 where the threshold is  $1.5\sigma$ . All four curves are plotted against the pulsar longitude in ms (upper scale) and degrees (lower scale).

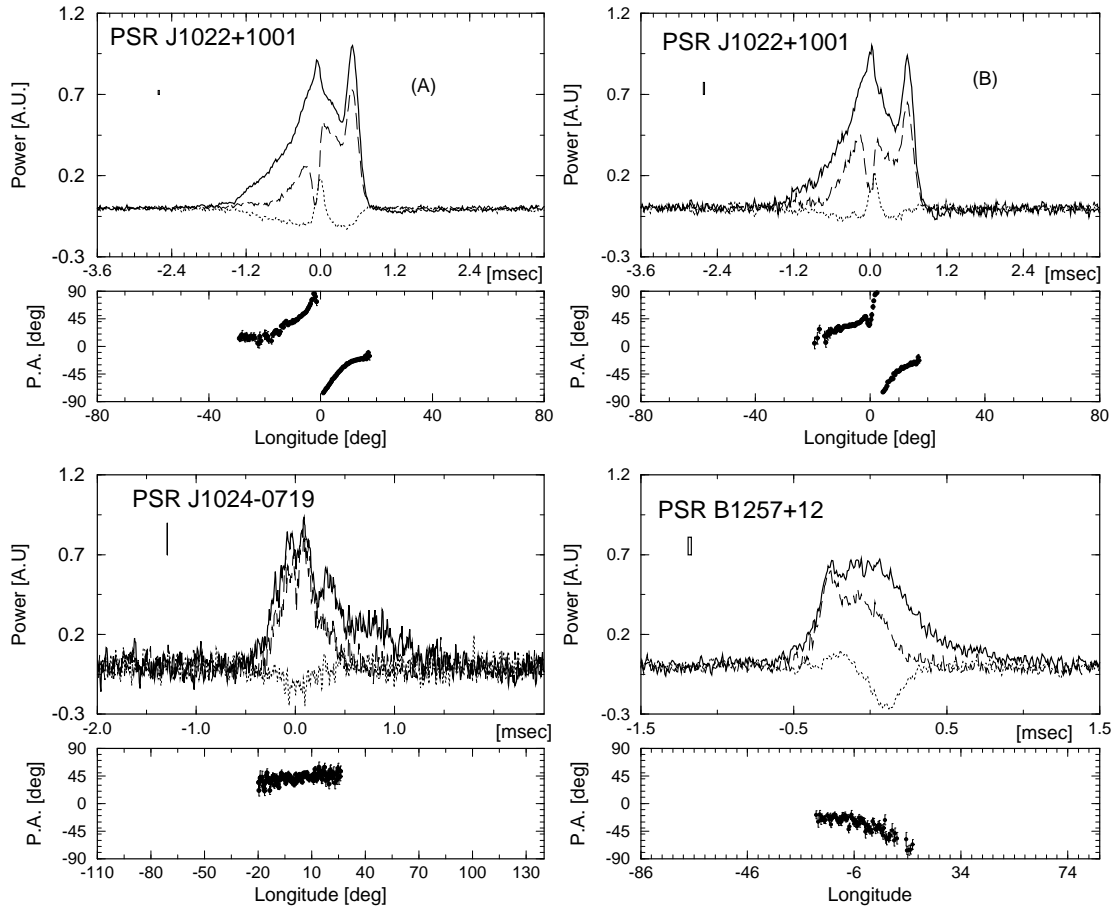


Fig. 2.— see Fig. 1

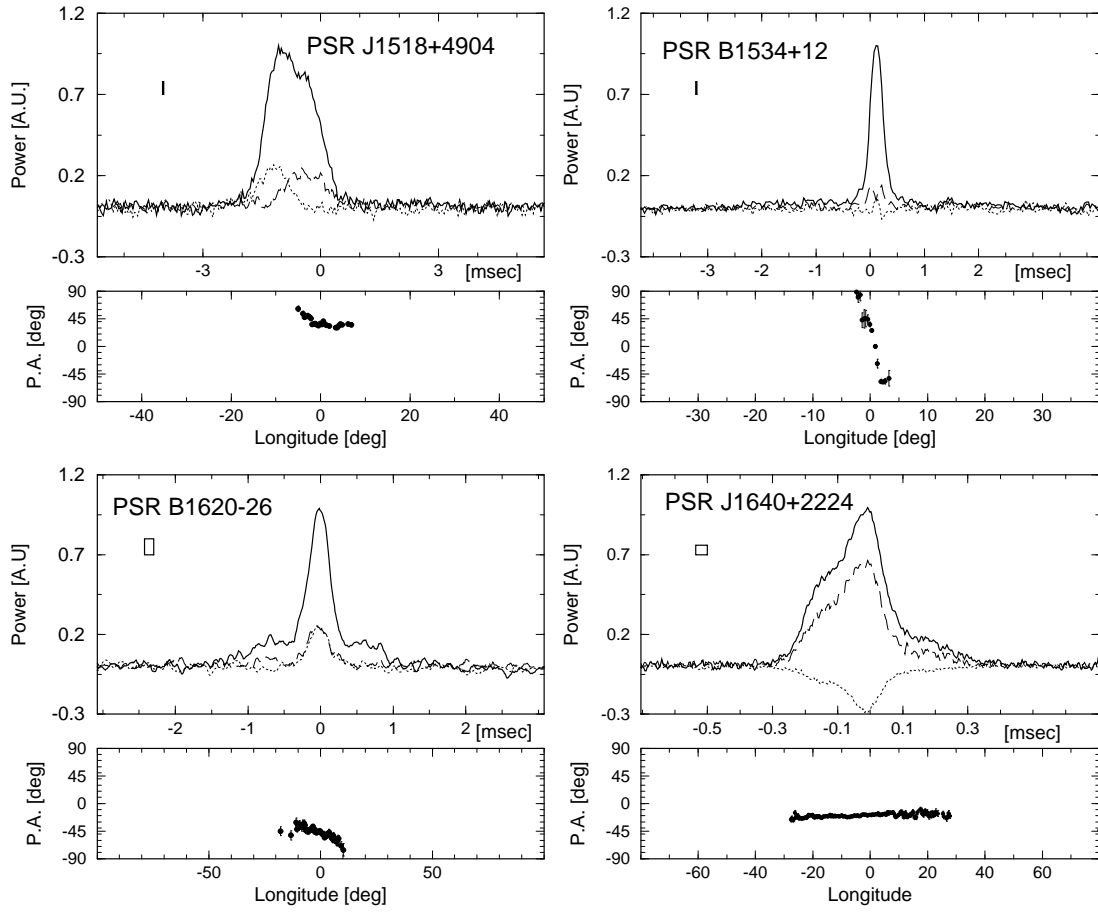


Fig. 3.— see Fig. 1

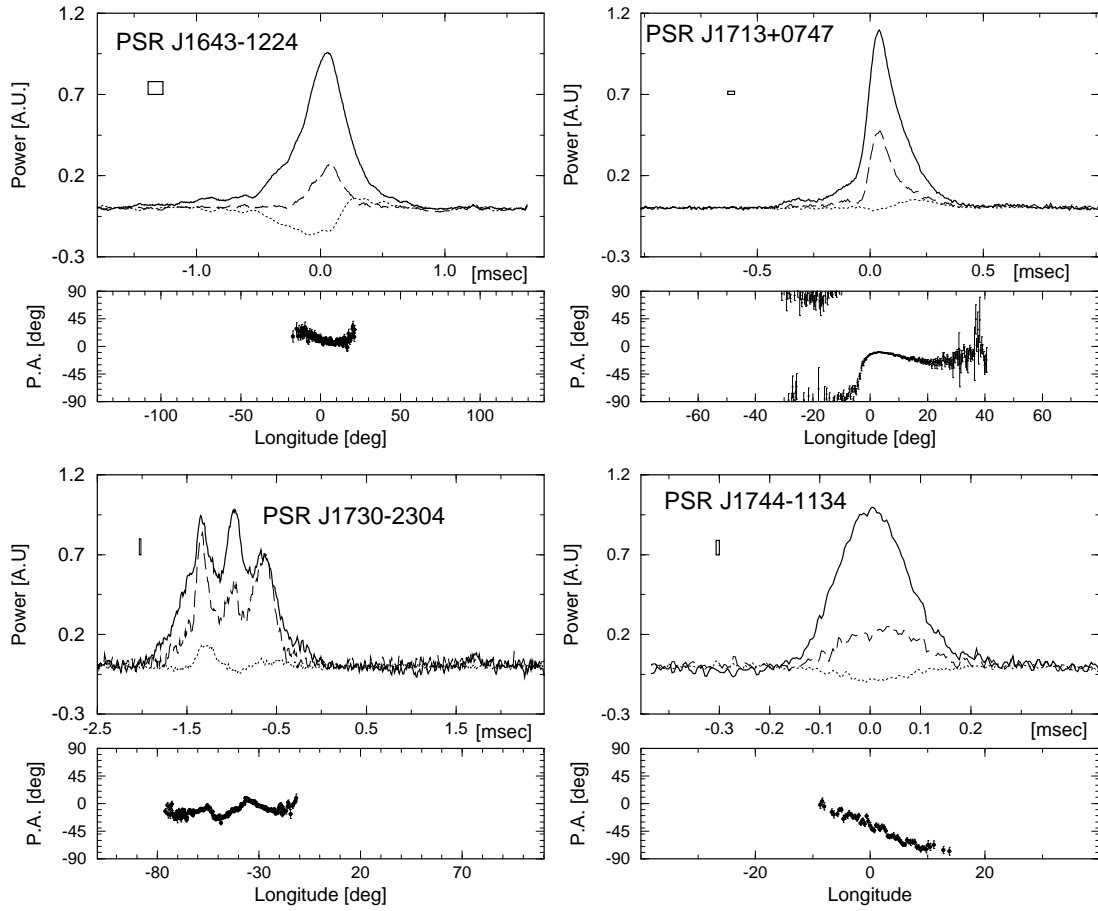


Fig. 4.— see Fig. 1



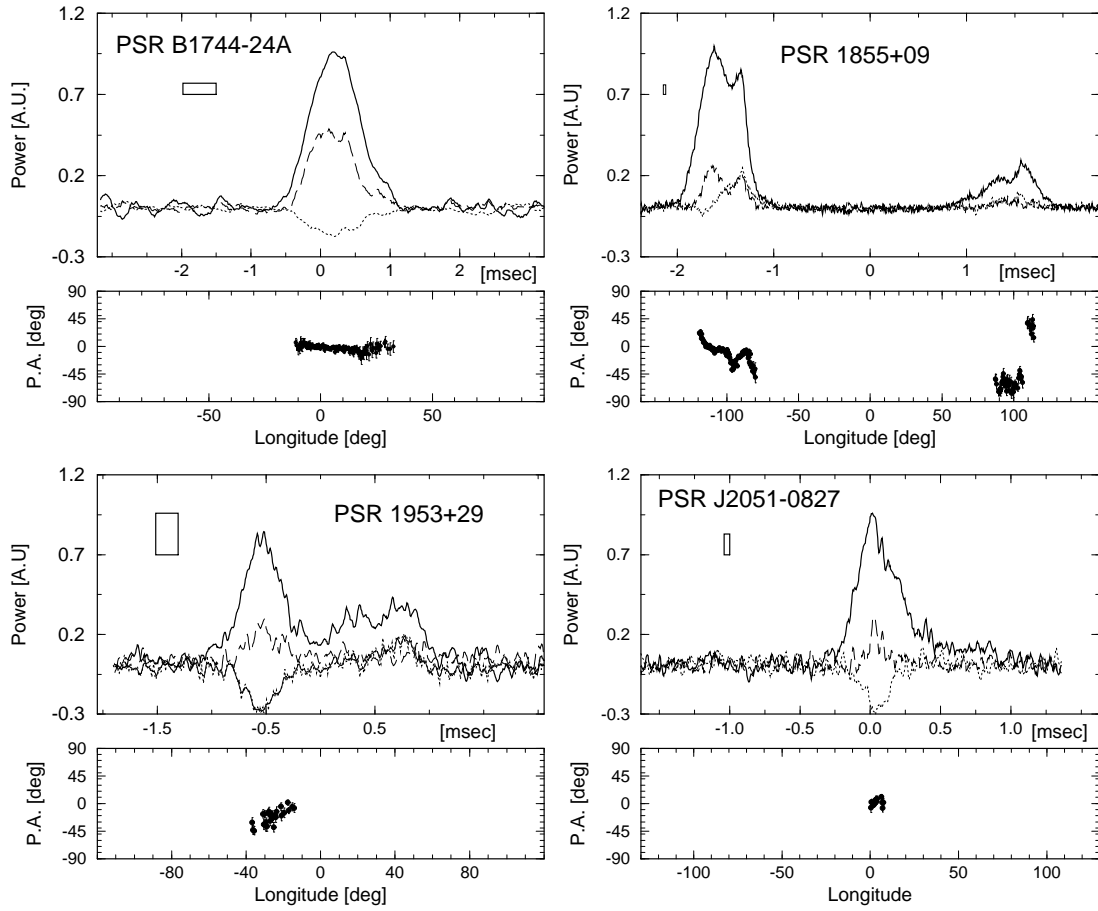


Fig. 5.— see Fig. 1

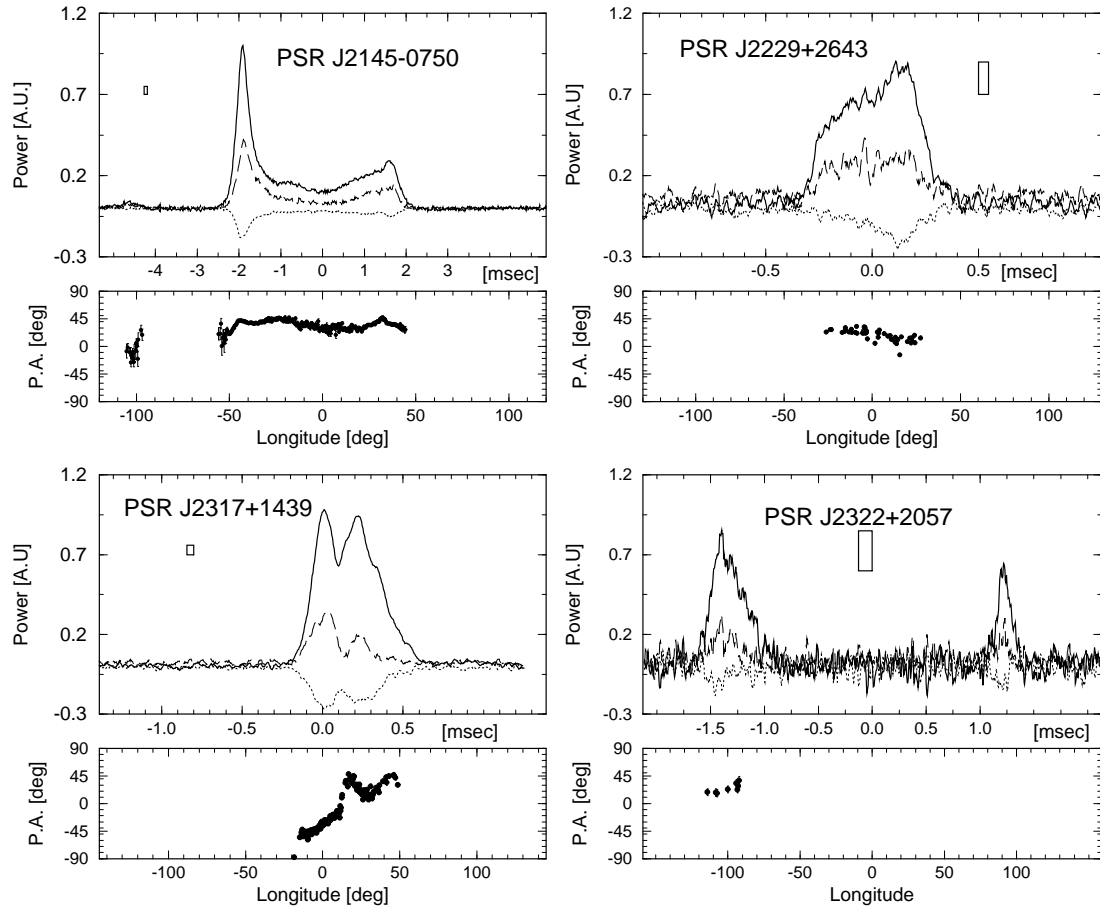


Fig. 6.— see Fig. 1

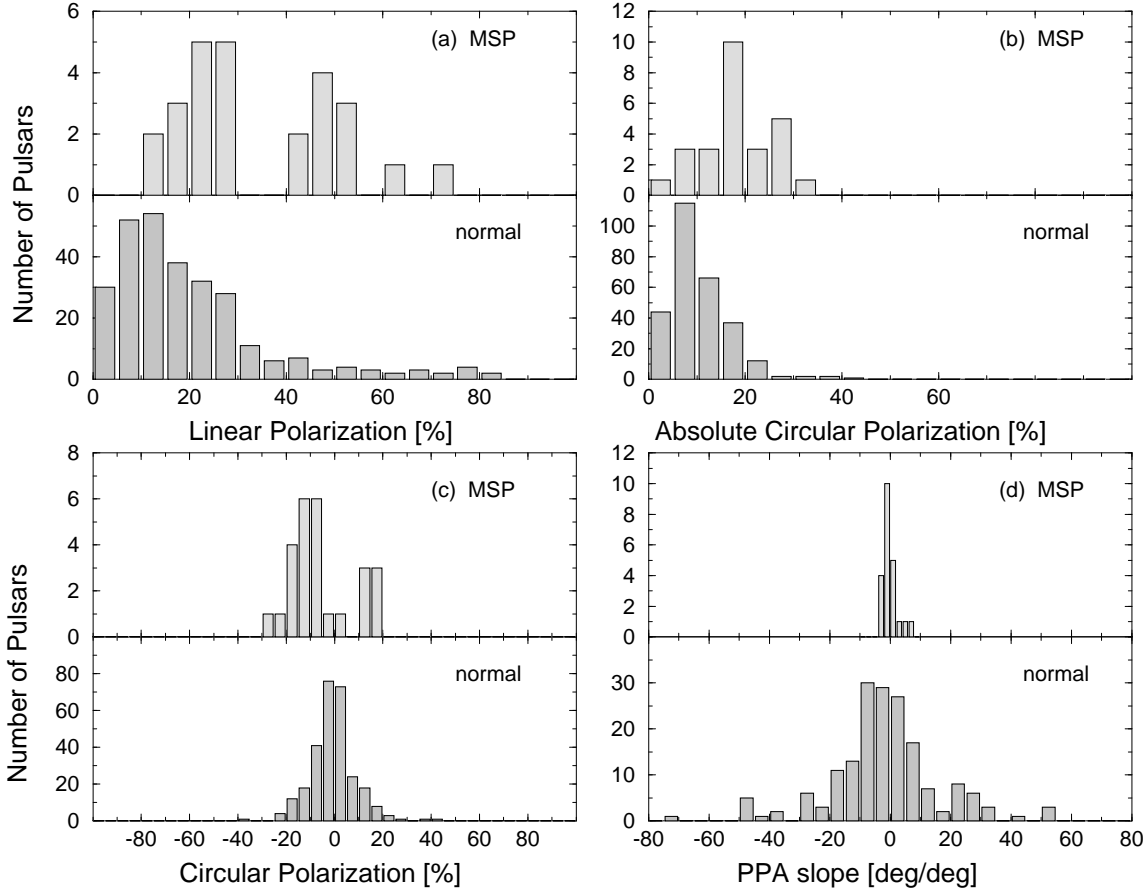


Fig. 7.— A statistical comparison of the emission properties between normal pulsars and MSPs. The histogram of the fractional linear (a), absolute circular (b) and circular (c) polarization is presented for 24 MSPs (upper panel) and 281 normal pulsars (lower panel). The polarization of the IPs of two MSPs in our sample is also considered in these histograms. In (d) the histogram of the steepest slope of the PPA curve for 20 MSPs in our sample and two from the literature is compared with the histogram for 178 normal pulsars.

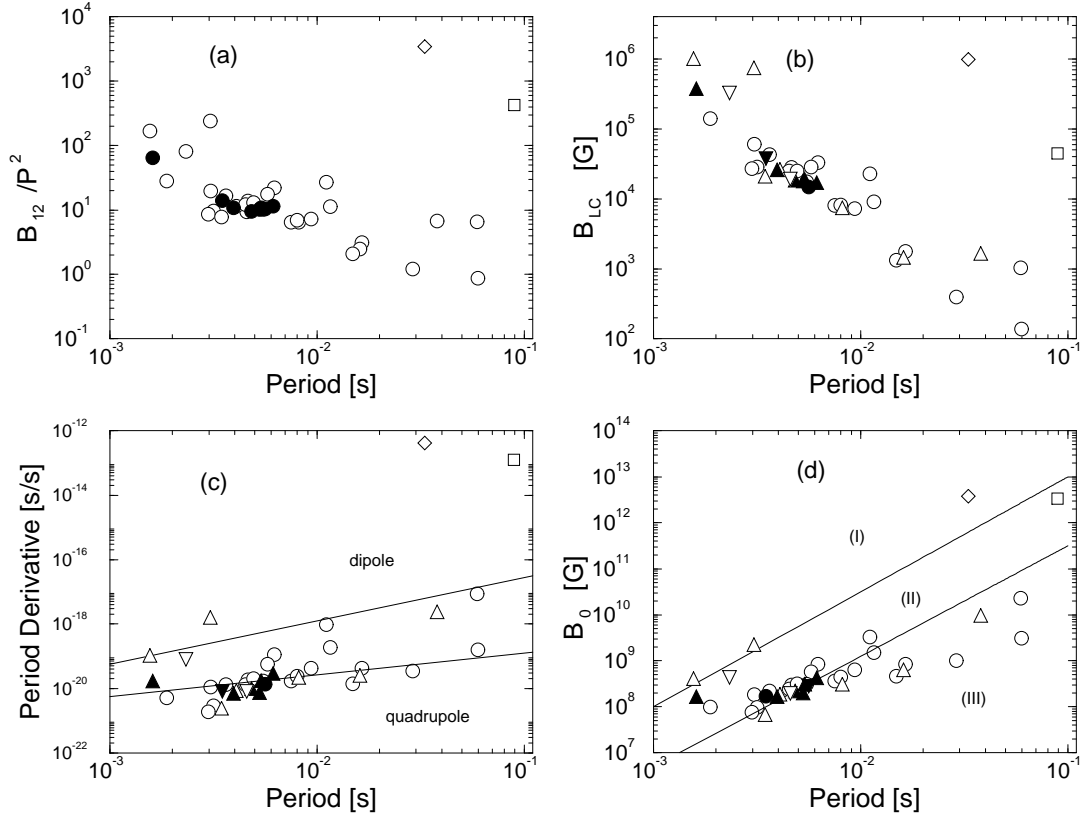


Fig. 8.— Physical parameters of MSPs versus pulse period. (a) accelerating potential, (b) dipolar magnetic field at the light cylinder, (c) period derivative and (d) dipolar component of the surface magnetic field. Filled symbols represent pulsars with abnormal profile development. In (b) – (d) MSPs with IPs and pre or post cursors are marked with triangles pointing up, while sources with extended emission are shown as triangles pointing down. In (c) dipole and quadrupole spin-up lines are superimposed, while in (d) the lines represent maximum locations of  $\gamma$ -ray emission (see text for details). For comparison, the Crab (diamond) and the Vela (square) pulsars are marked.

Table 1. Polarization parameters for 24 MSPs. The mean fractional polarization (linear, absolute circular and circular) and the associated errors are presented in cols. 2, 3, and 4 respectively. The maximum slope of the PPA curve is presented in column 5

PSR	$\frac{L}{T}$ (%)	$ \frac{V}{T} $ (%)	$\frac{V}{T}$ (%)	$\left(\frac{d\psi}{d\phi}\right)_{\max}$ $\left(\frac{\text{deg}}{\text{deg}}\right)$
J0613–0200	26.3 ± 2.1	16.2 ± 1.1	–12.7 ± 1.1	...
J0621+1002	14.7 ± 1.5	7.6 ± 1.3	–6.7 ± 1.3	...
J0751+1807	28.5 ± 1.5	12.7 ± 1.0	–9.3 ± 1.0	1.86 ± 0.19
J1012+5307	54.8 ± 0.7	18.4 ± 0.6	–11.3 ± 1.0	–2.70 ± 0.09
J1022+1001	52.8 ± 0.4	15.7 ± 0.4	–12.6 ± 0.4	6.12 ± 0.20
J1024–0719	47.8 ± 1.7	18.3 ± 1.4	–9.6 ± 0.4	0.34 ± 0.03
B1257+12	51.7 ± 2.9	25.0 ± 2.7	–17.8 ± 2.7	–1.17 ± 0.08
J1518+4904	21.7 ± 1.7	19.5 ± 1.7	16.5 ± 1.7	–1.32 ± 0.21
B1534+12	17.9 ± 2.7	15.1 ± 4.5	–5.1 ± 4.5	–2.00 ± 0.19
B1620–26	20.8 ± 1.6	21.0 ± 1.6	13.5 ± 1.6	–1.52 ± 0.10
J1640+2224	70.3 ± 0.8	27.1 ± 0.4	–21.9 ± 0.4	0.17 ± 0.02
J1643–1224	22.8 ± 1.0	21.3 ± 0.8	–10.8 ± 0.7	–1.10 ± 0.06
J1713+0747	29.7 ± 0.2	15.5 ± 0.2	15.3 ± 0.2	–1.70 ± 0.04
J1730–2304	60.9 ± 1.0	4.7 ± 0.5	10.4 ± 0.4	2.23 ± 0.09
B1744–1134	26.8 ± 1.7	9.6 ± 1.3	–9.1 ± 1.3	–3.70 ± 0.12
B1744–24A	46.1 ± 2.0	12.3 ± 1.3	–8.2 ± 1.5	–0.40 ± 0.03
B1855+09MP	19.5 ± 0.5	13.6 ± 0.5	12.3 ± 0.5	–1.67 ± 0.07
B1855+09IP	15.8 ± 1.7	22.2 ± 1.9	18.0 ± 1.9	–1.14 ± 0.48
B1937+21MP	24.6 ± 0.1	6.5 ± 0.1	0.1 ± 0.1	...
B1937+21IP	46.9 ± 0.1	11.3 ± 0.1	–0.5 ± 0.1	...
B1953+29	25.7 ± 2.8	27.7 ± 1.6	–5.3 ± 2.2	1.38 ± 0.19
J2051–0827	11.9 ± 2.1	25.6 ± 2.1	–13.7 ± 2.2	–1.36 ± 0.49
J2145–0750	45.1 ± 0.3	17.7 ± 0.2	–17.6 ± 0.2	–0.65 ± 0.04
J2229+2643	42.3 ± 2.6	17.6 ± 1.0	–15.3 ± 1.5	–0.55 ± 0.08
J2317+1439	24.1 ± 0.8	25.7 ± 0.4	–25.7 ± 0.9	1.65 ± 0.06
J2322+2057MP	27.6 ± 4.6	16.7 ± 3.8	–12.1 ± 3.5	...
J2322+2057IP	41.6 ± 4.6	34.7 ± 3.8	–15.1 ± 3.5	...

Table 2. Physical Parameters of MSPs.

PSR	$P$ (ms)	$B$ ( $10^8$ G)	$\left(\frac{B_{12}}{P^2}\right)$	$\left(\frac{1}{Q}\right)$	$R_{\text{LC}}$ (km)	$R_{\text{cap}}$ (km)	$m_2$ ( $M_{\odot}$ )	Profile evolution
J0613–0200	3.062	1.86	19.83	3.03	146.2	2.71	0.15	M/A?
J0621+1002	28.854	10.17	1.22	0.41	1377.7	0.88	0.54	M
J0751+1807	3.479	1.69	13.95	2.32	166.1	2.54	0.15	A
J1012+5307	5.256	2.80	10.15	1.87	251.0	2.07	0.13	A
J1022+1001	16.453	8.41	3.11	0.81	785.6	1.17	0.87	N
J1024–0719	5.612	3.25	10.32	1.91	268.0	2.00	...	A
B1257+12	6.219	8.49	21.96	3.53	296.9	1.90	...	M/N
J1518+4904	40.935	...	...	...	1954.5	0.74	1.01	M
B1534+12	37.904	97.12	6.76	1.65	1809.8	0.77	1.34	N
B1620–26	11.076	33.18	27.04	4.41	528.9	1.43	...	M
J1640+2224	3.163	0.97	9.69	1.71	151.0	2.67	0.30	M
J1643–1224	4.621	2.96	13.86	2.37	220.6	2.21	0.14	M
J1713+0747	4.570	1.96	9.36	1.73	218.2	2.22	0.33	N
J1730–2304	8.123	4.25	6.44	1.36	387.9	1.66	...	M
J1744–1134	4.075	1.89	11.41	2.00	194.6	2.35	...	M
B1744–24A	11.564	15.00	11.22	2.19	552.2	1.39	...	M
B1855+09	5.362	3.13	10.89	1.98	256.0	2.05	0.26	A
B1913+16	59.030	228.36	6.55	1.68	2818.5	0.62	1.39	N
B1937+21	1.558	4.10	168.70	15.70	74.4	3.80	...	M
B1957+20	1.607	1.66	64.38	7.29	76.7	3.74	0.03	A
B1953+29	6.133	4.30	11.44	2.09	292.8	1.92	0.21	A
J2019+2425	3.935	1.68	10.86	1.92	187.9	2.39	0.37	A
J2051–0827	4.509	2.45	12.05	2.11	215.3	2.23	0.03	M
J2145–0750	16.052	6.41	2.49	0.68	766.4	1.18	0.51	M
J2229+2643	2.978	0.76	8.58	1.55	142.2	2.75	0.15	M
J2317+1439	3.445	0.92	7.79	1.45	164.5	2.56	0.21	N
J2322+2057	4.808	2.19	9.47	1.75	229.6	2.16	...	A